Supplementary Information for

Synthesis, structure and reactivity of iridium(III) complexes containing a bis-cyclometalated tridentate C^N^C ligand

Wai-Man Cheung,[a] Man-Chun Chong,[a] Herman H.-Y. Sung,[a] Shun-Cheung Cheng,[b] Ian D. Williams,*[a] Chi-Chiu Ko*[b] and Wa-Hung Leung*[a]

[a]Department of Chemistry, The Hong Kong University of Science and Technology, Clear Water Bay, Kowloon, China. E-mail: chwill@ust.hk, chleung@ust.hk.

[b]Department of Chemistry, City University of Hong Kong, Tat Chee Avenue, Kowloon, Hong Kong, China. E-mail: vinccko@cityu.edu.hk

Table of Content

Table S1. Crystallographic data and experimental details for **2**, **3**, **4**, **5**, **8**, **8'**, **9** and **10**.

	2	**3**	**4**	**5**	**8**	**8'**	**9**	**10**
Formula	$C_{42}H_{54}Cl_5HgIr_2N \cdot CH_2Cl_2$	$C_{41}H_{51}Cl_2HgIr_2N$	$C_{33}H_{39}ClHgIrN \cdot (CH_2Cl_2)_{1.375}$	$C_{33}H_{39}ClIrN \cdot CH_3OH$	$C_{51}H_{55}IrN_2O$	$C_{51}H_{55}IrN_2O \cdot C_6H_{14}$	$C_{58}H_{63}IrN_2O_4S$	$C_{54}H_{43}ClIrP_3 \cdot (CH_2Cl_2)_{0.5}$
Formula weight	1335.10	1213.71	1026.98	709.34	904.17	990.34	1076.36	1054.90
Crystal system	triclinic	triclinic	monoclinic	triclinic	monoclinic	monoclinic	triclinic	triclinic
Space group	P-1	P-1	$P2_1/n$	P-1	$P2_1/c$	$P2_1/c$	P-1	P-1
a, Å	11.4169(5)	10.6104(4)	21.7337(2)	12.0649(4)	11.78531(10)	14.19411(12)	10.3452(4)	10.7955(5)
b, Å	11.6904(5)	12.0252(5)	11.72515(11)	12.2041(5)	12.98197(13)	13.27153(11)	15.7451(6)	12.1139(4)
c, Å	16.8087(7)	16.6227(8)	29.5201(3)	12.5489(6)	28.0763(2)	26.6663(2)	16.1341(6)	18.5808(6)
α, deg	70.906(4)	69.278(4)	90	118.782(5)	90	90	94.912(3)	76.851(3)
β, deg	79.811(3)	72.867(4)	104.7030(11)	105.993(4)	91.5588(8)	92.5650(8)	99.262(3)	88.011(3)
γ, deg	88.663(3)	83.902(3)	90	100.339(3)	90	90	105.162(3)	69.189(4)
V, Å^3	2085.12(16)	1895.69(15)	7276.30(13)	1445.99(12)	4293.99(7)	5018.30(7)	2480.87(17)	2208.99(15)
Z	2	2	8	2	4	4	2	2
ρ_{calc}, g cm^{-3}	2.126	2.126	1.875	1.629	1.399	1.311	1.441	1.586
T, K	100.01(10)	173.00(10)	100.00(10)	100.00(10)	173.00(10)	173.00(10)	173.00(10)	118(20)
μ, mm^{-1}	21.753	21.942	17.162	9.986	6.304	5.438	5.981	8.280
F(000)	1264.0	1144.0	3956.0	712.0	1840.0	2040.0	1100.0	1054.0
Total reflections	11532	10545	39147	8101	16314	31708	16355	12789
Independent reflections	7357	7056	13080	5132	8191	10304	10011	8465
R_{int}	0.0255	0.0245	0.0326	0.0220	0.0250	0.0229	0.0287	0.0274
GoF^a	1.046	1.011	1.039	1.011	1.020	1.035	1.035	1.026
R_1,^{b} wR_2^{c} [$I > 2\sigma(I)$]	0.0340, 0.0860	0.0245, 0.0625	0.0334, 0.0805	0.0207, 0.0521	0.0233, 0.0546	0.0210, 0.0514	0.0257, 0.0620	0.0299, 0.0758
R_1, wR_2 (all data)	0.0361, 0.0876	0.0262, 0.0637	0.0394, 0.0830	0.0216, 0.0526	0.0267, 0.0565	0.0233, 0.0530	0.0280, 0.0638	0.0325, 0.0775

^{a} GoF = $[\Sigma w(|F_o| - |F_c|)^2/(N_{obs} - N_{param})]^{½}$. ^{b} $R_1 = \Sigma||F_o| - |F_c||/\Sigma|F_o|$. ^{c} wR_2 $[(\Sigma w|F_o| - |F_c|)^2/\Sigma w^2|F$

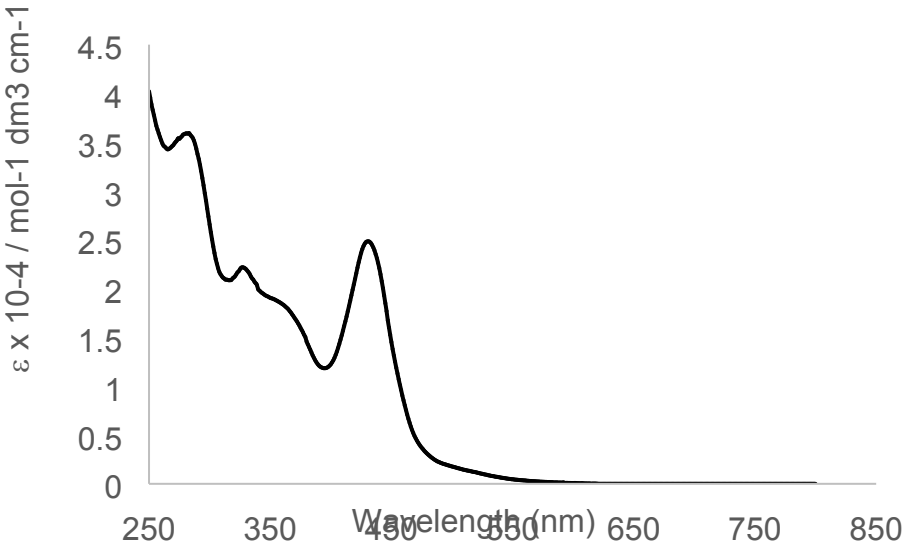

Figure S1. UV-visible spectrum of [Cl(κ^2-HC^N^C)(cod)IrHgIr(cod)Cl_2]$_2$ (**2**) in CH_2Cl_2 at room temperature.

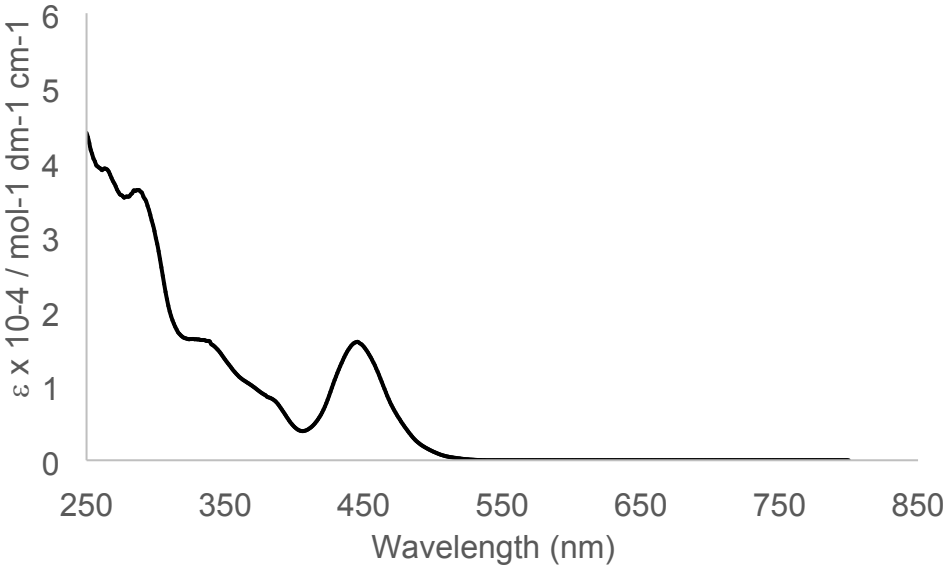

Figure S2. UV-visible spectrum of [(C^N^C)(cod)IrHgIr(cod)Cl_2] (**3**) in CH_2Cl_2 at room temperature.

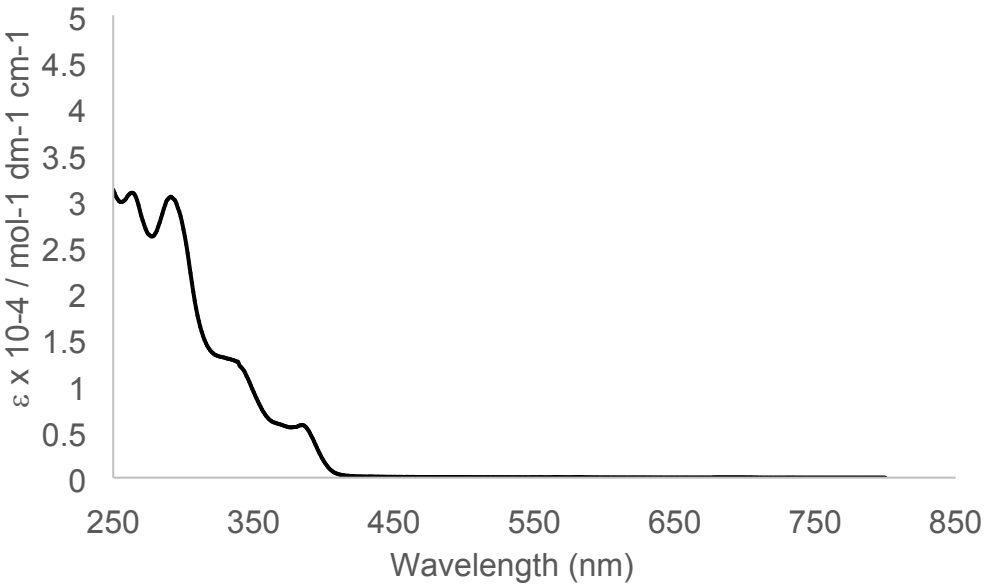

Figure S3. UV-visible spectrum of [Ir(C^N^C)(cod)(HgCl)] (**4**) in CH_2Cl_2 at room temperature.

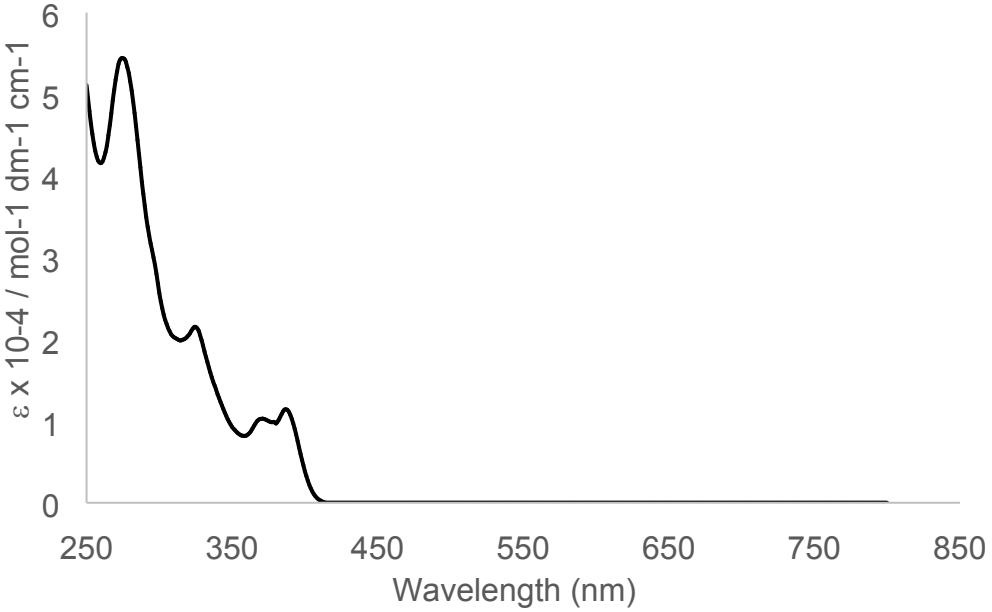

Figure S4. UV-visible spectrum of [Ir(C^N^C)(cod)Cl·$HgCl_2$] (**5·$HgCl_2$**) in CH_2Cl_2 at room temperature.

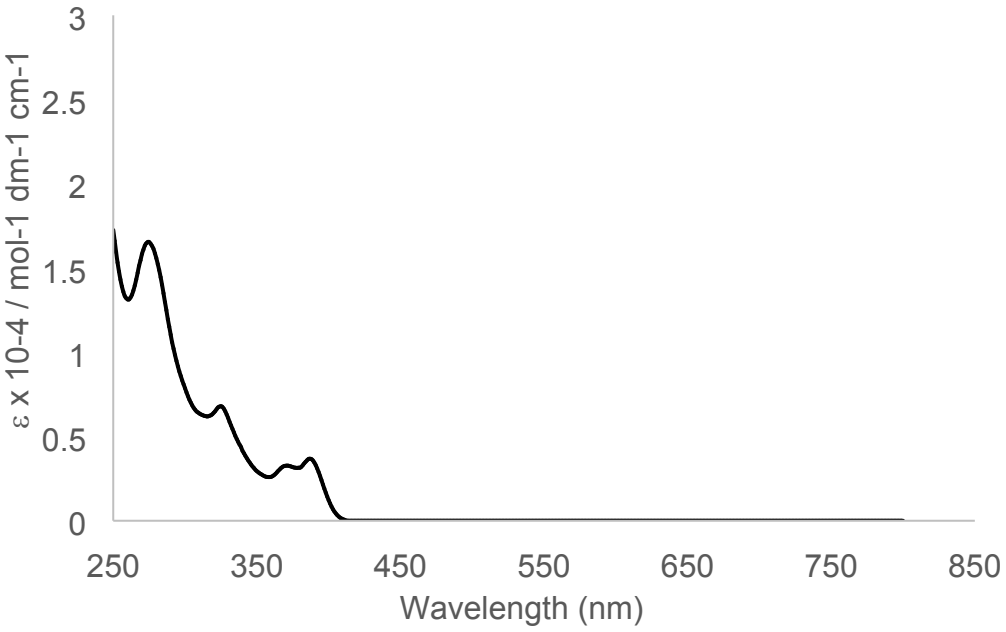

Figure S5. UV-visible spectrum of [Ir(C^N^C)(cod)Cl] (**5**) in CH_2Cl_2 at room temperature.

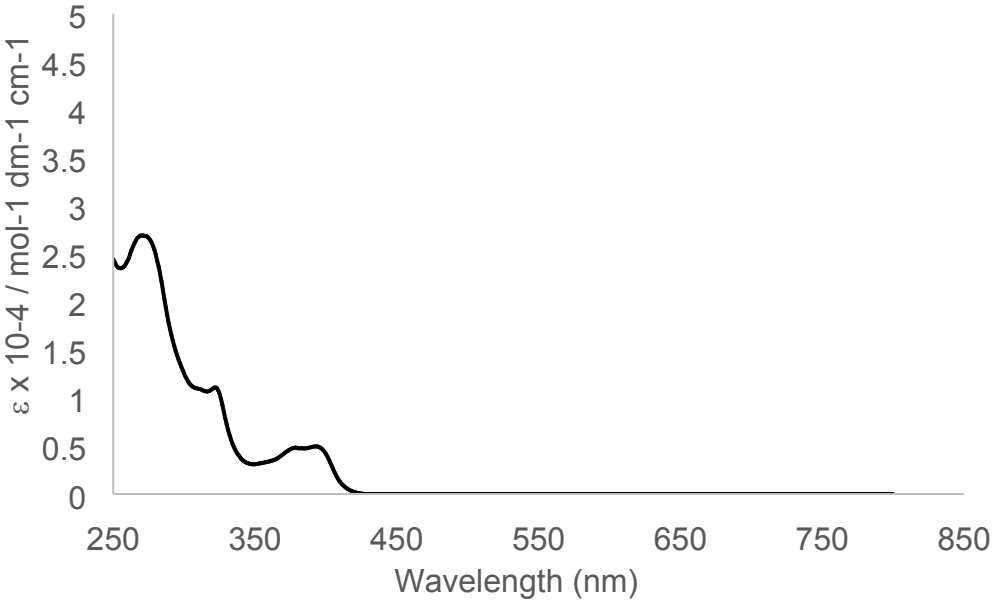

Figure S6. UV-visible spectrum of [Ir(C^N^C)(cod)(H_2O)][OTf] (**6**) in CH_2Cl_2 at room temperature.

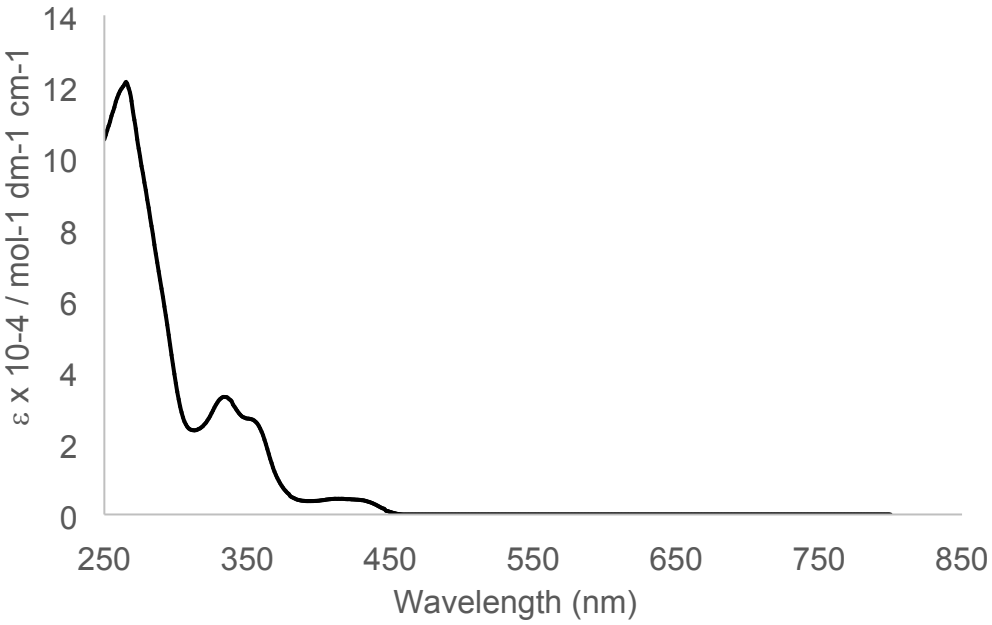

Figure S7. UV-visible spectrum of [Ir(C^N^C)(HgCl)(CO)(py)] (**7**) in CH_2Cl_2 at room temperature.

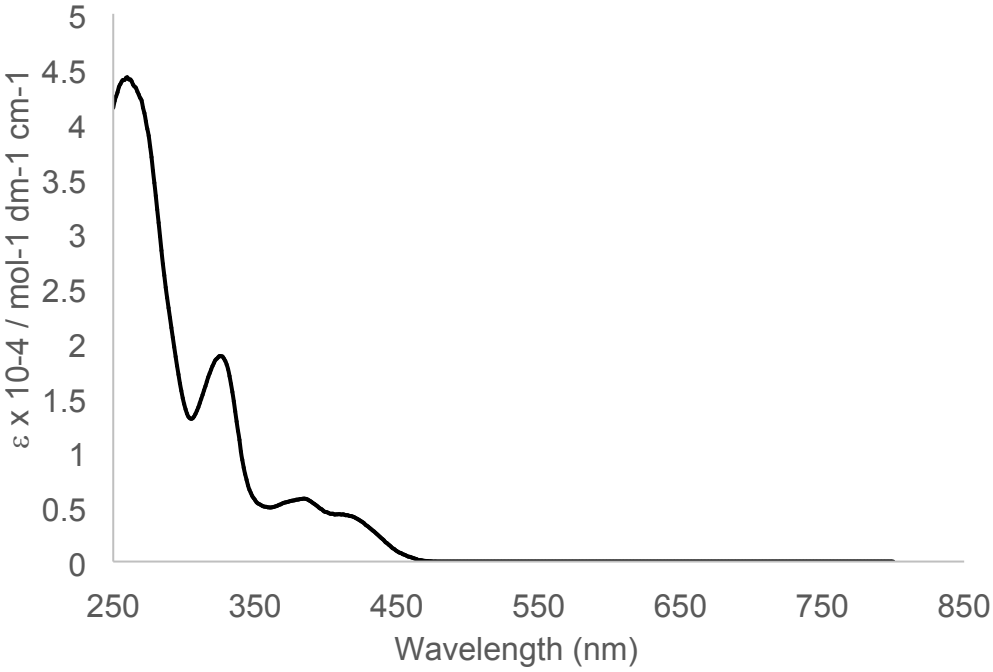

Figure S8. UV-visible spectrum of [Ir(C^N^C)(κ^2-HC^N^C)(CO)] (**8**) in CH_2Cl_2 at room temperature.

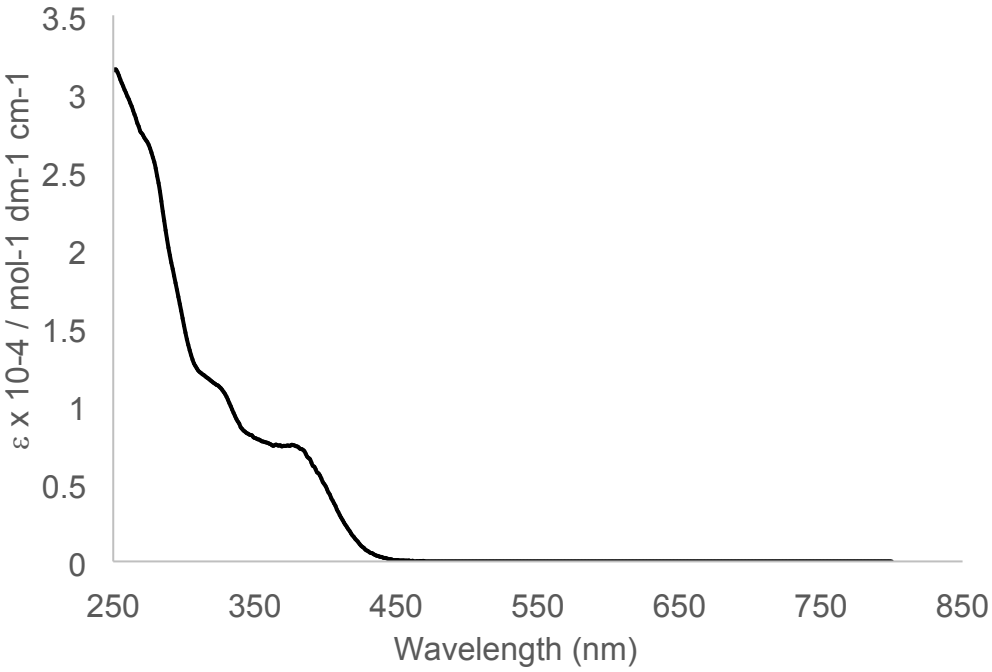

Figure S9. UV-visible spectrum of **8'** in CH_2Cl_2 at room temperature.

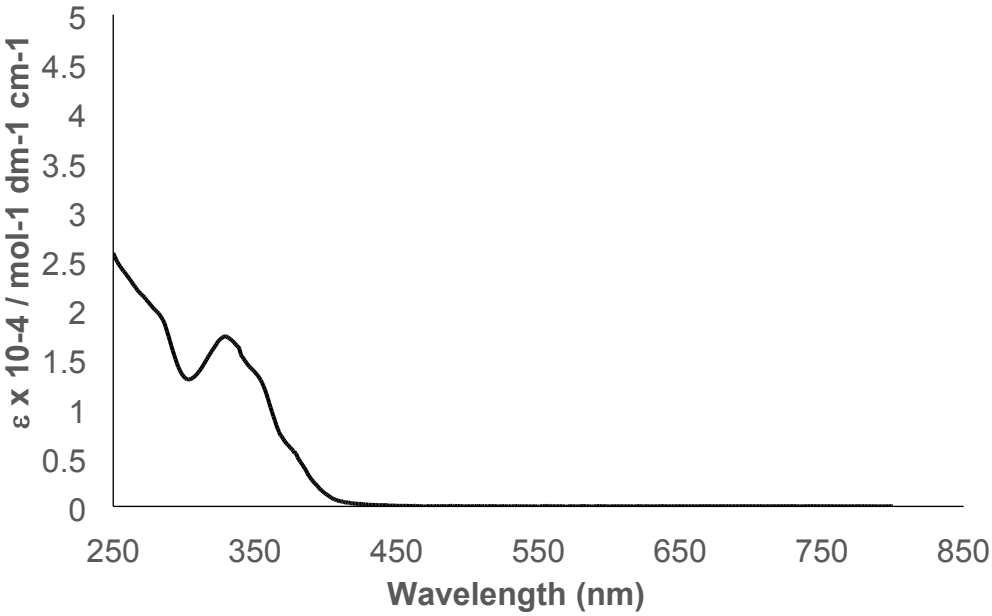

Figure S10. UV-visible spectrum of [Ir(κ^2-HC^N^C)$_2$(OTs)(CO)] (**9**) in CH_2Cl_2 at room temperature.

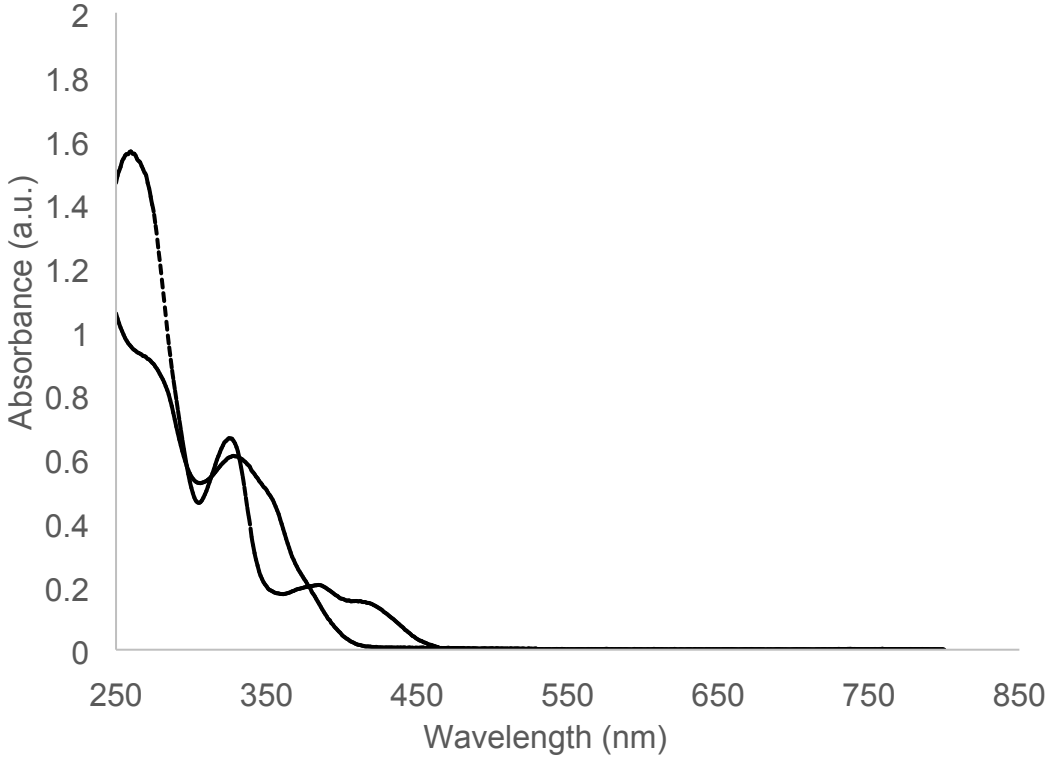

Figure S11. UV-visible spectra of **8** (dashed line) and the product of oxidation of **8** with $(4\text{-}BrC_6H_4)_3NSbCl_6$ (solid line) in CH_2Cl_2.

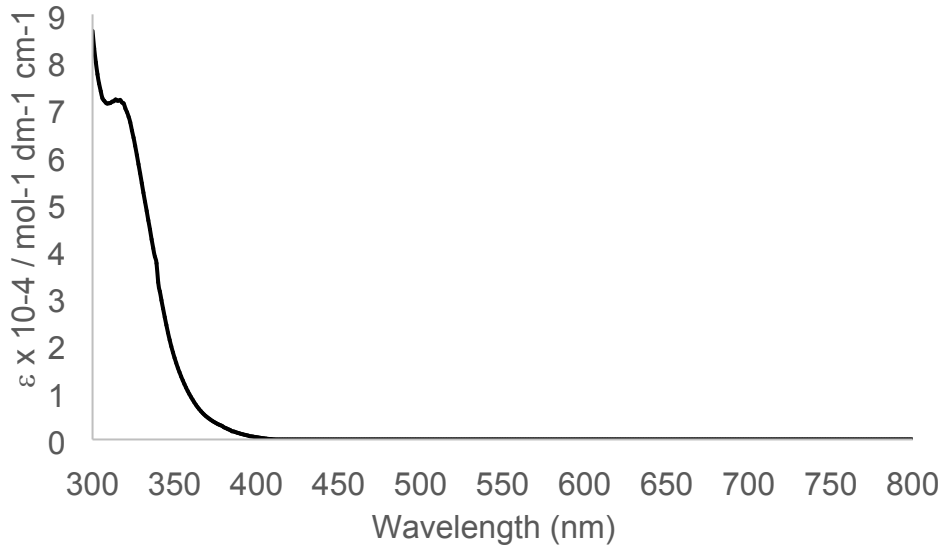

Figure S12. UV-visible spectrum of $[Ir(PPh_3)(\kappa^2\text{-}P,C\text{-}C_6H_4PPh_2)_2Cl]$ (**10**) in CH_2Cl_2.

Emission Spectra

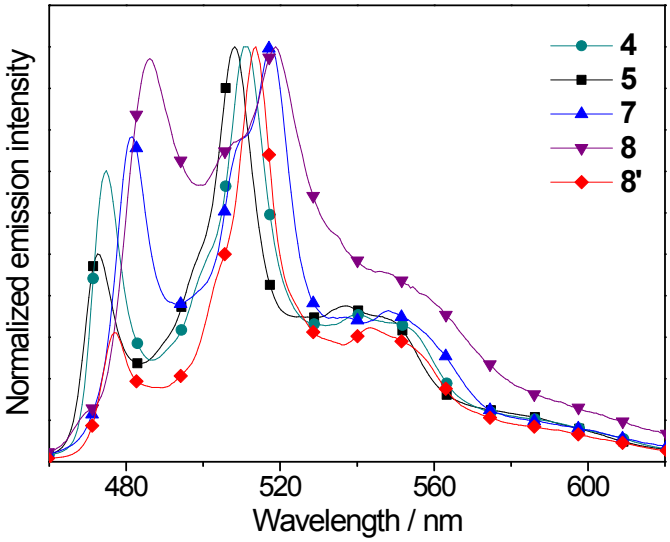

Figure S13. Overlaid normalized emission spectra of **4**, **5**, **7**, **8** and **8'** in 77 K EtOH-MeOH (4:1, v/v) glassy medium.

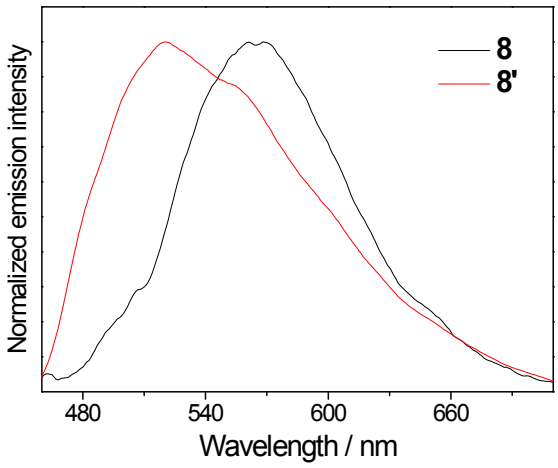

Figure S14. Overlaid emission spectra of [Ir(C^N^C)(κ^2-HC^N^C)(CO)] (**8**) and its isomer (**8'**) in 298 K CH_2Cl_2 solution.

FT-IR spectra

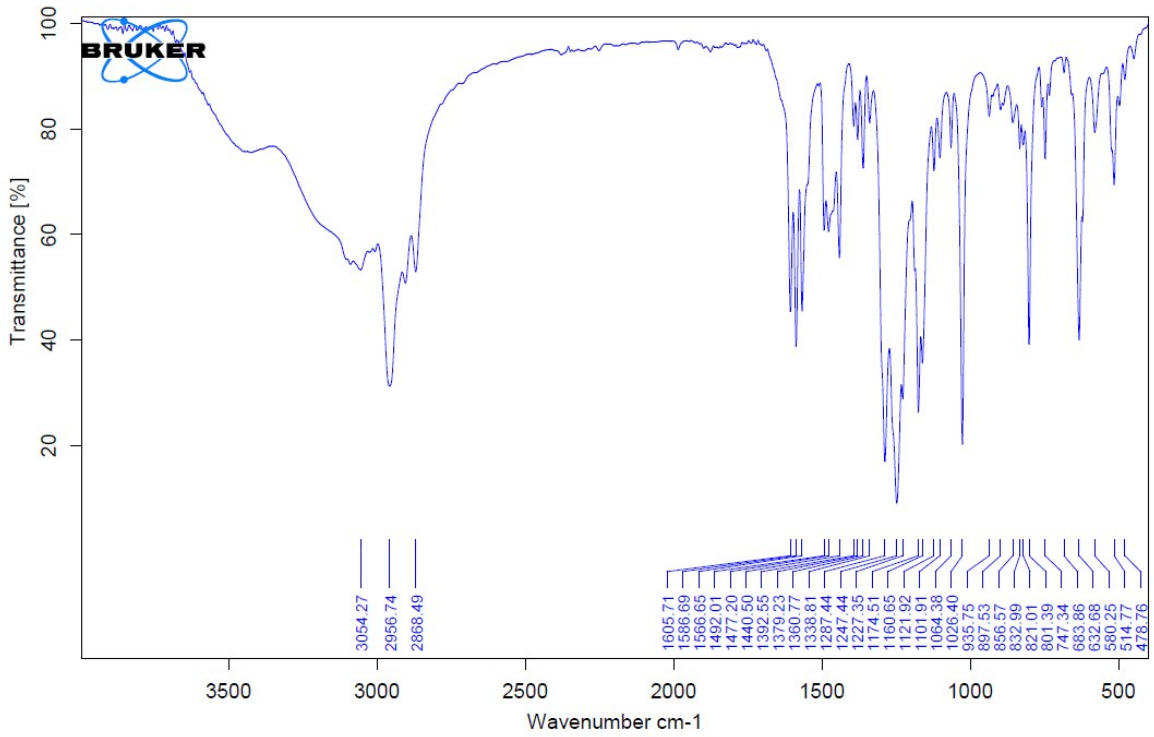

Figure S15. FT-IR (KBr) spectrum of [Ir(C^N^C)(cod)(H_2O)](OTf) (**6**).

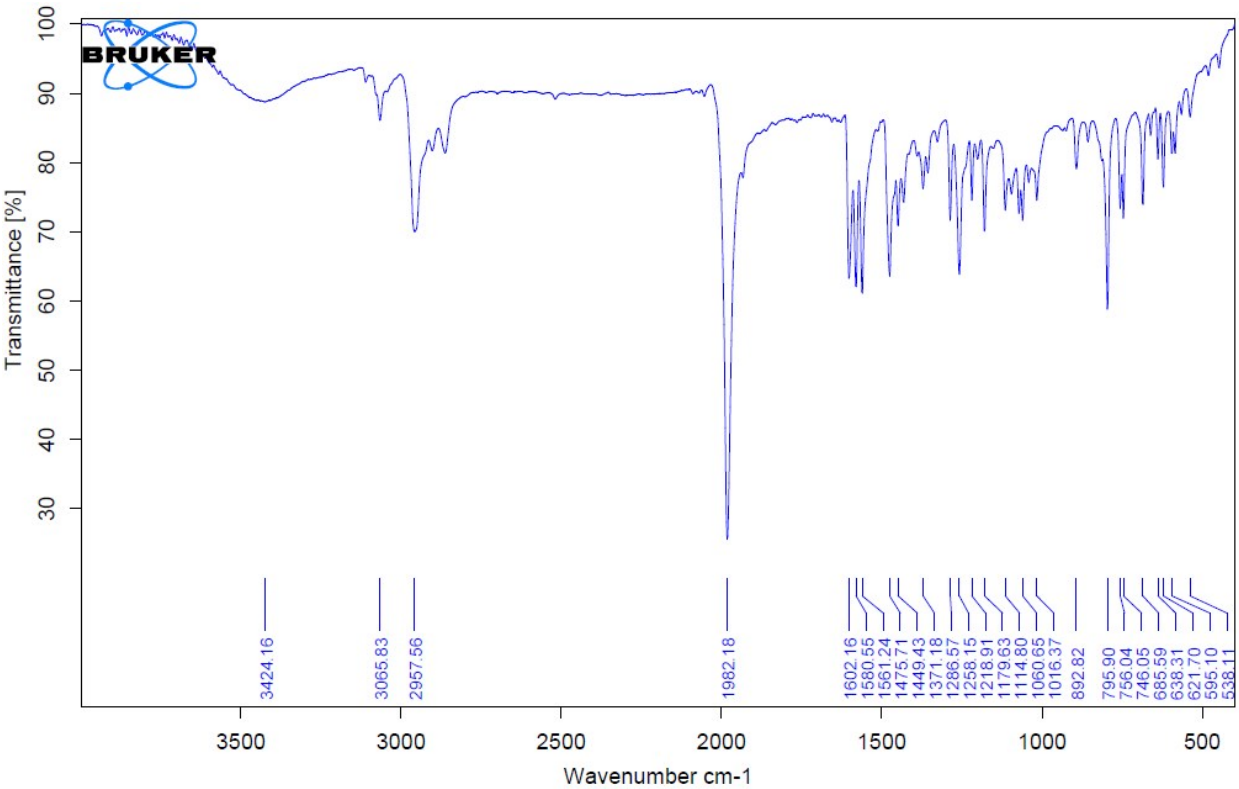

Figure S16. FT-IR (KBr) spectrum of [Ir(C^N^C)(HgCl)(CO)(py)] (**7**).

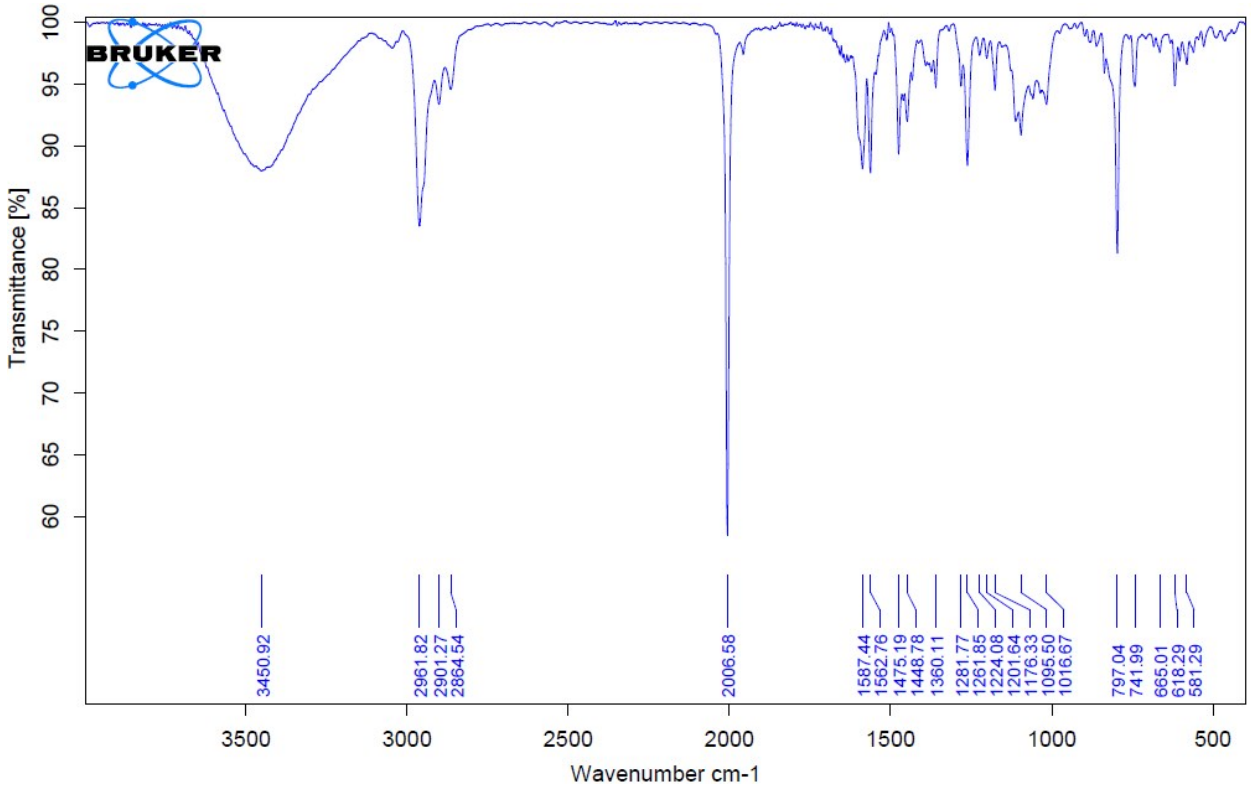

Figure S17. FT-IR (KBr) spectrum of [Ir(CNC)(κ^2-HC^N^C)(CO)] (**8**).

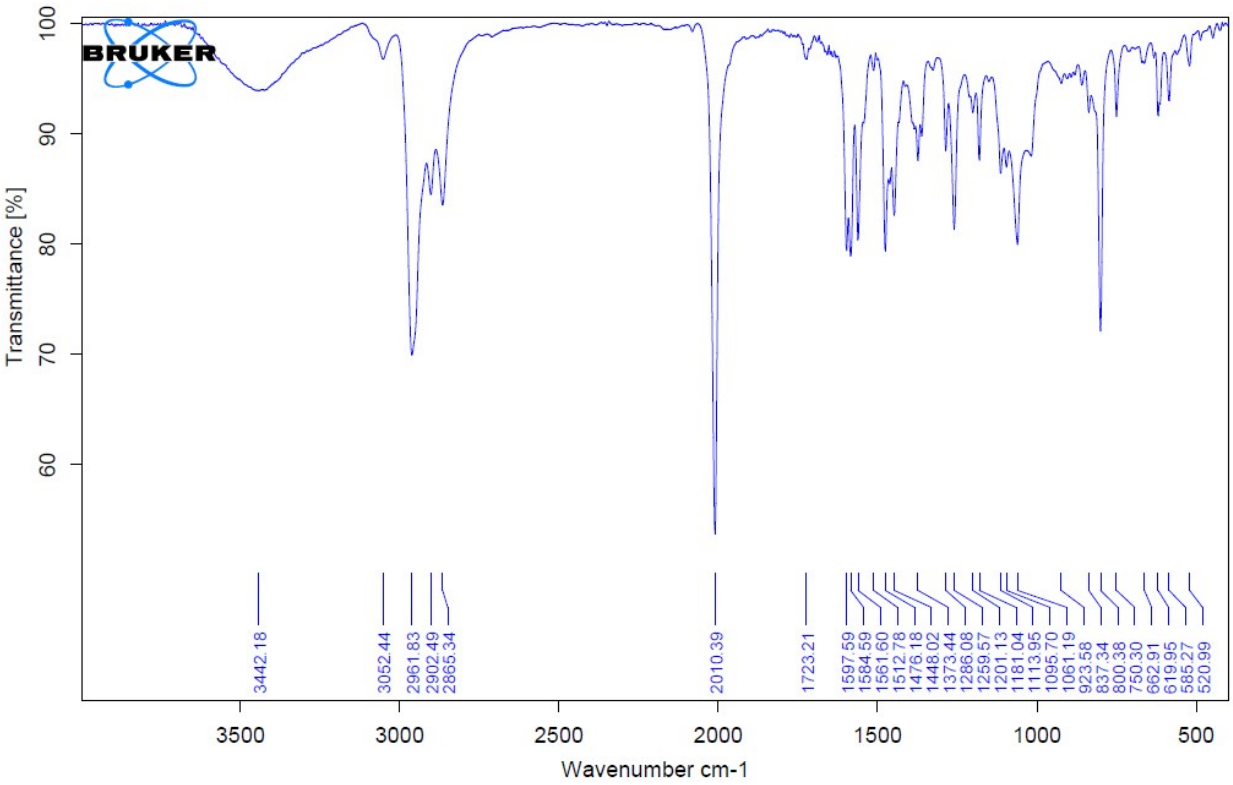

Figure S18. FT-IR (KBr) spectrum of **8'**.

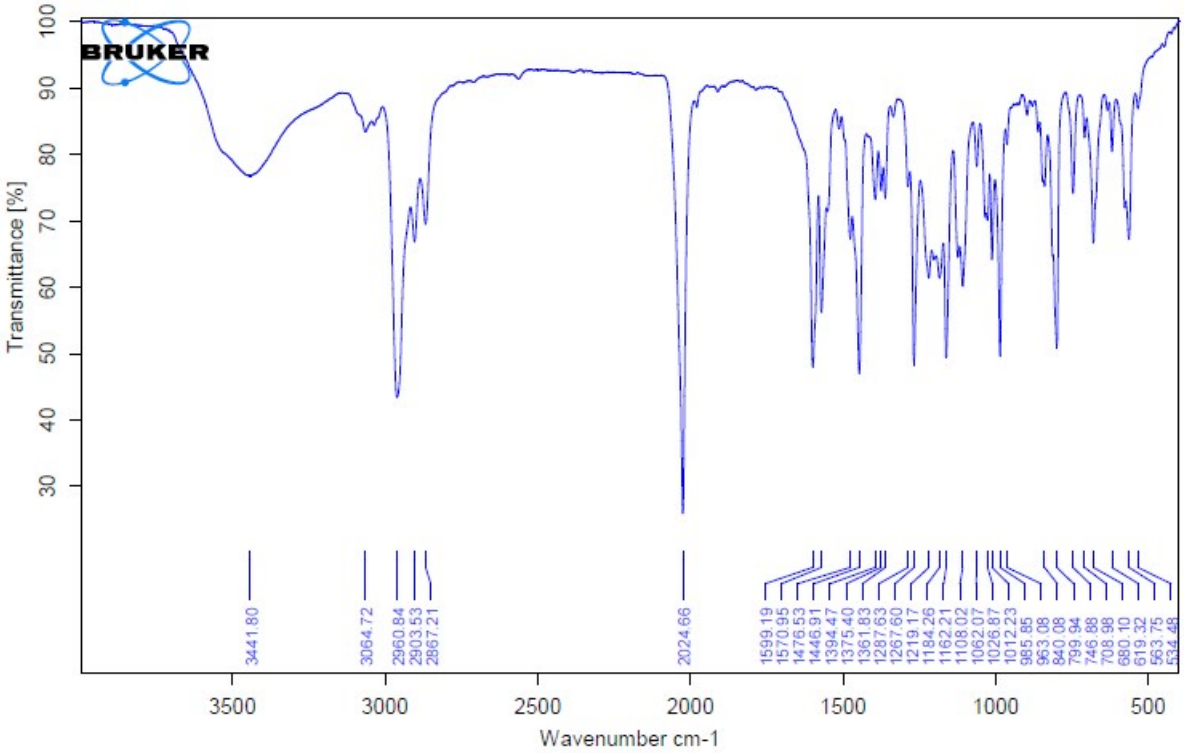

Figure S19. FT-IR (KBr) spectrum of **9**.

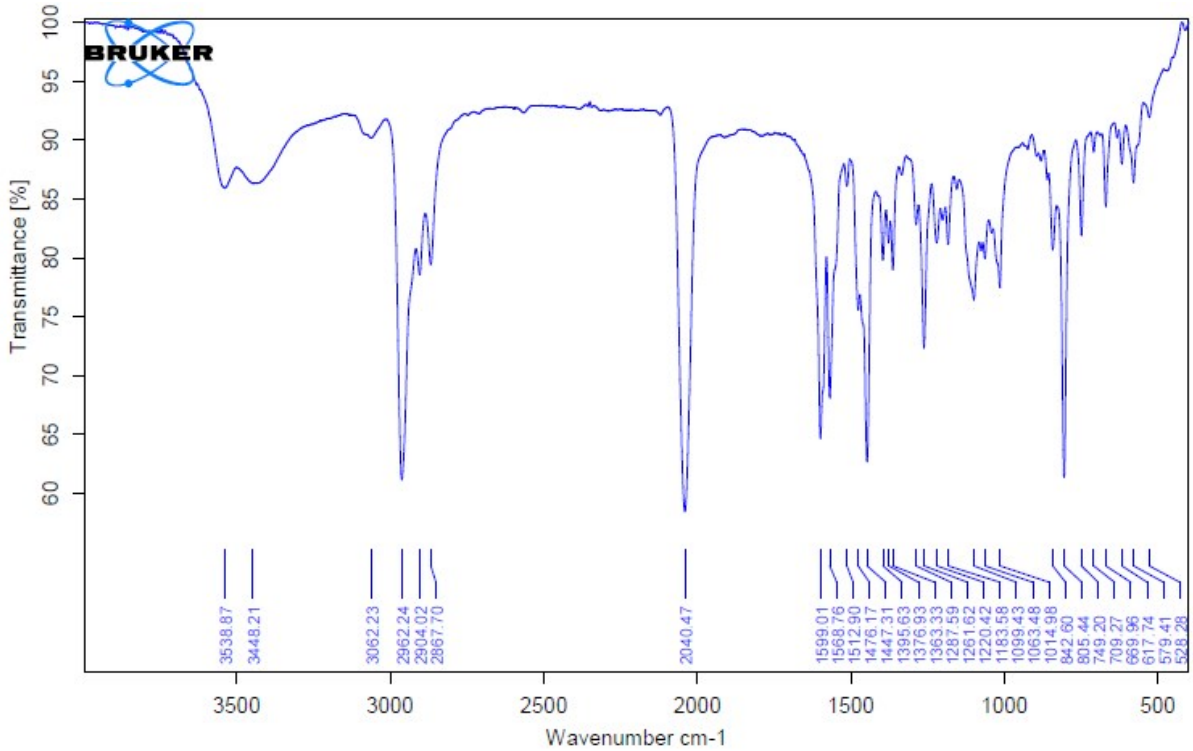

Figure S20. FT-IR (KBr) spectrum of the product of oxidation **8** by $(Br\text{-}C_6H_4)_3NSbCl_6$

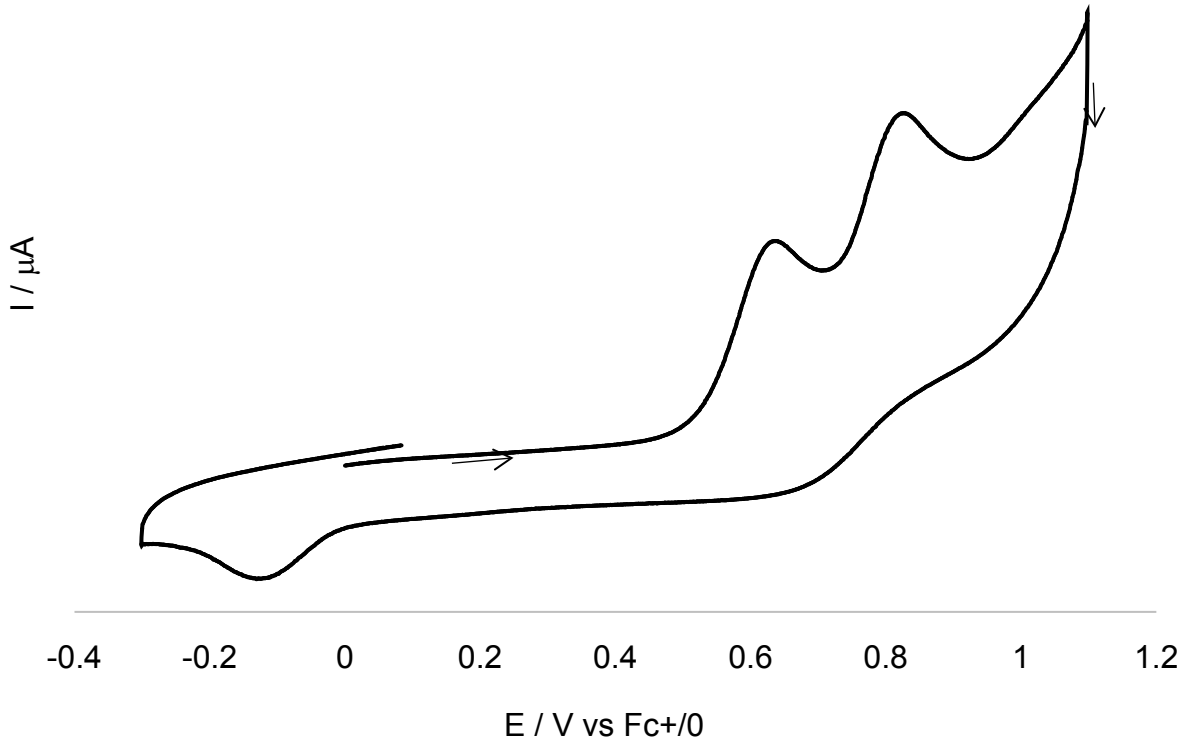

Figure S21. Cyclic voltammogram of **5** in CH_2Cl_2 with 0.2 M [*n*Bu_4N]PF_6 as supporting electrolyte (working electrode: glassy carbon, scan rate = 100 mV s^{-1}).

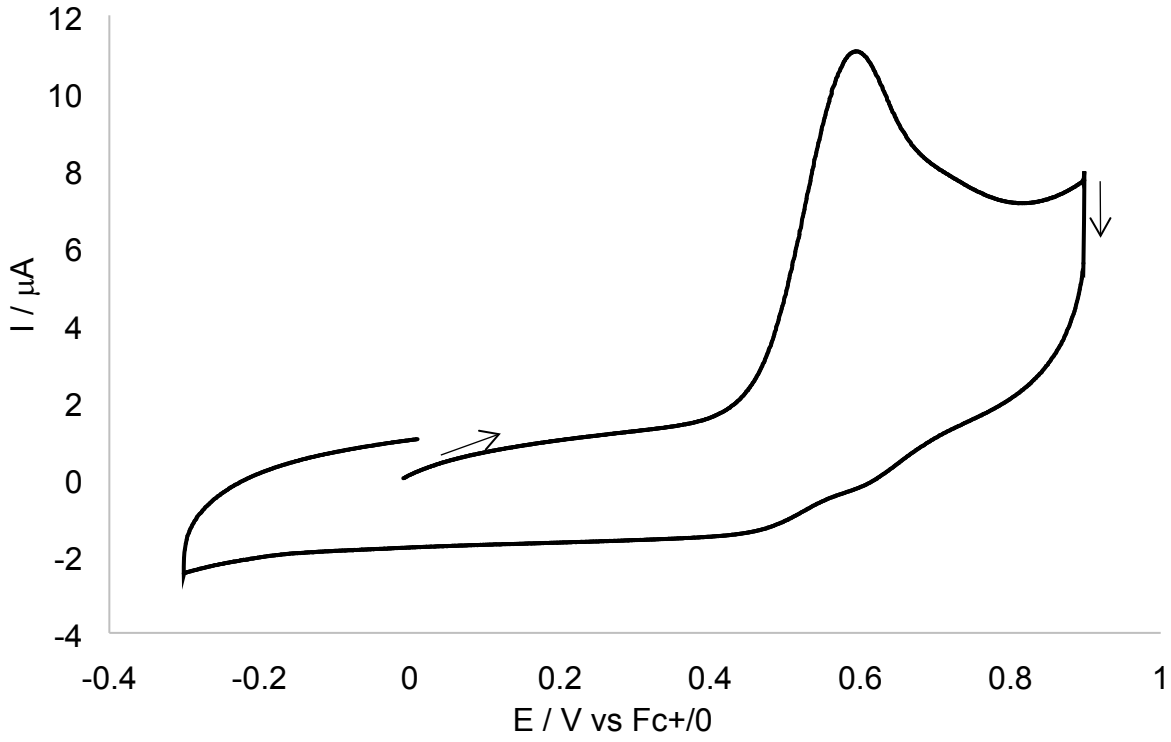

Figure S22. Cyclic voltammogram of **7** in CH_2Cl_2 with 0.2 M [*n*Bu_4N]PF_6 as supporting electrolyte (working electrode: glassy carbon, scan rate = 100 mV s^{-1}).

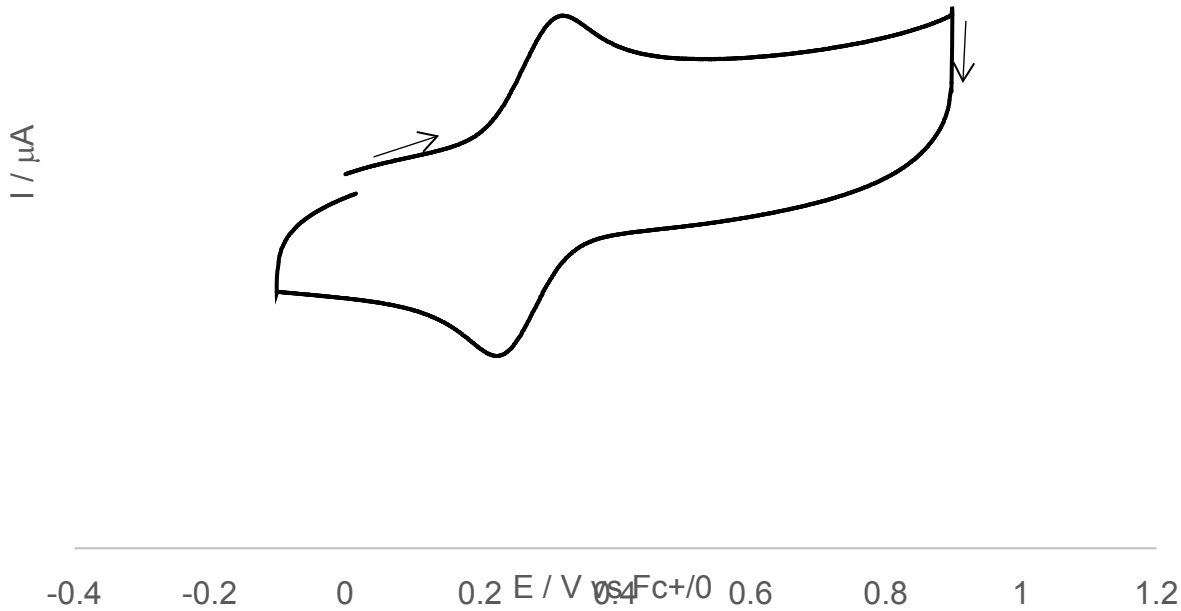

Figure S23. Cyclic voltammogram of **8** in CH_2Cl_2 with 0.2 M [*n*Bu_4N]PF_6 as supporting electrolyte (working electrode: glassy carbon, scan rate = 100 mV s^{-1}).

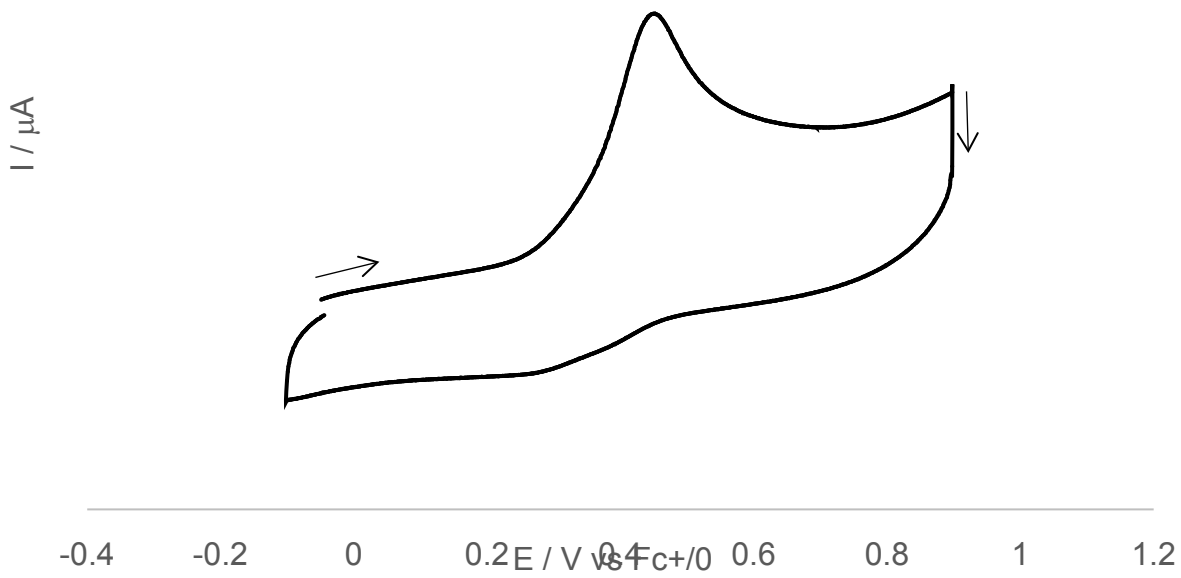

Figure S24. Cyclic voltammogram of **8'** in CH_2Cl_2 with 0.2 M [*n*Bu_4N]PF_6 as supporting electrolyte (working electrode: glassy carbon, scan rate = 100 mV s^{-1}).

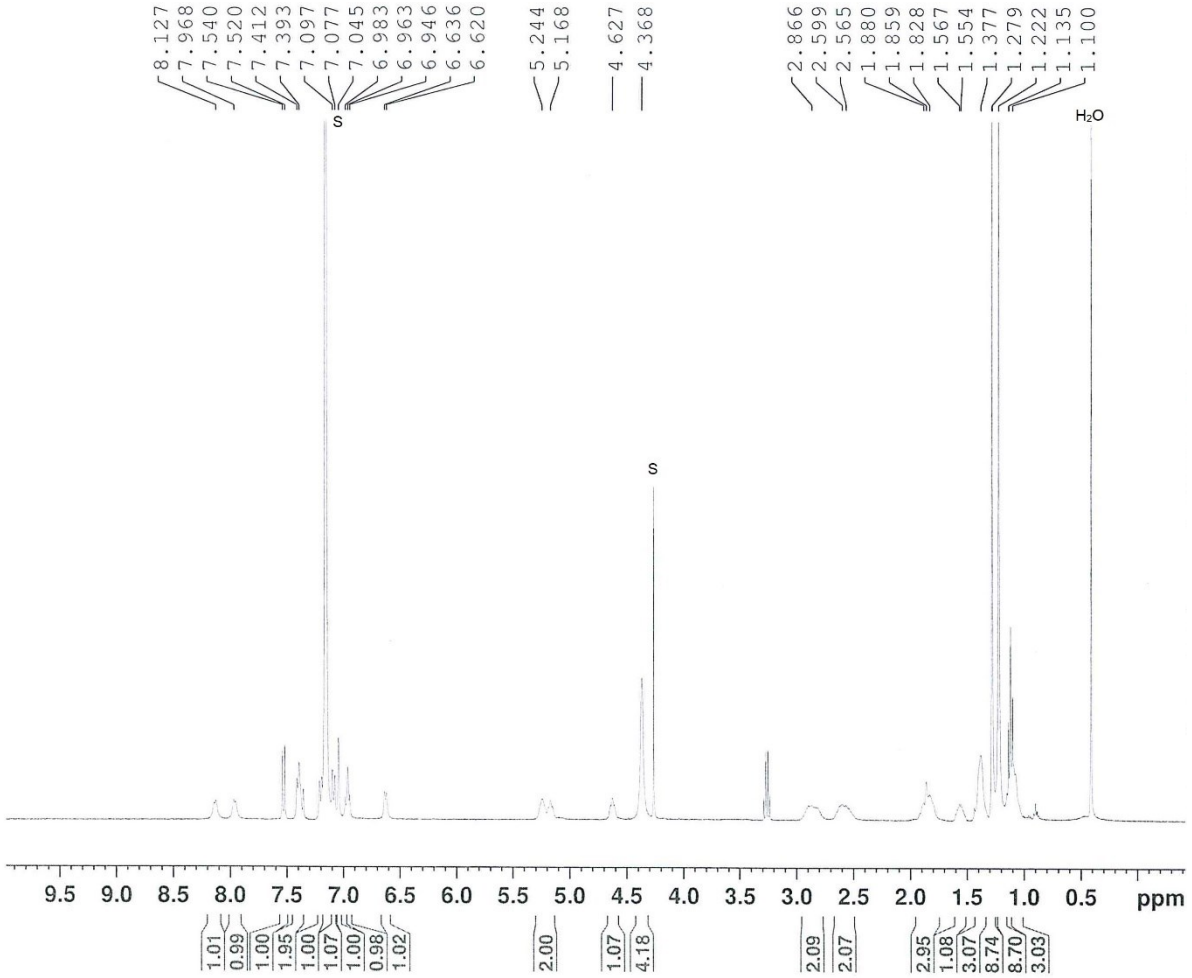

Figure S25. ^{1}H NMR (400 MHz, 298 K, C_6D_6) spectrum of **2** (S = residual solvent).

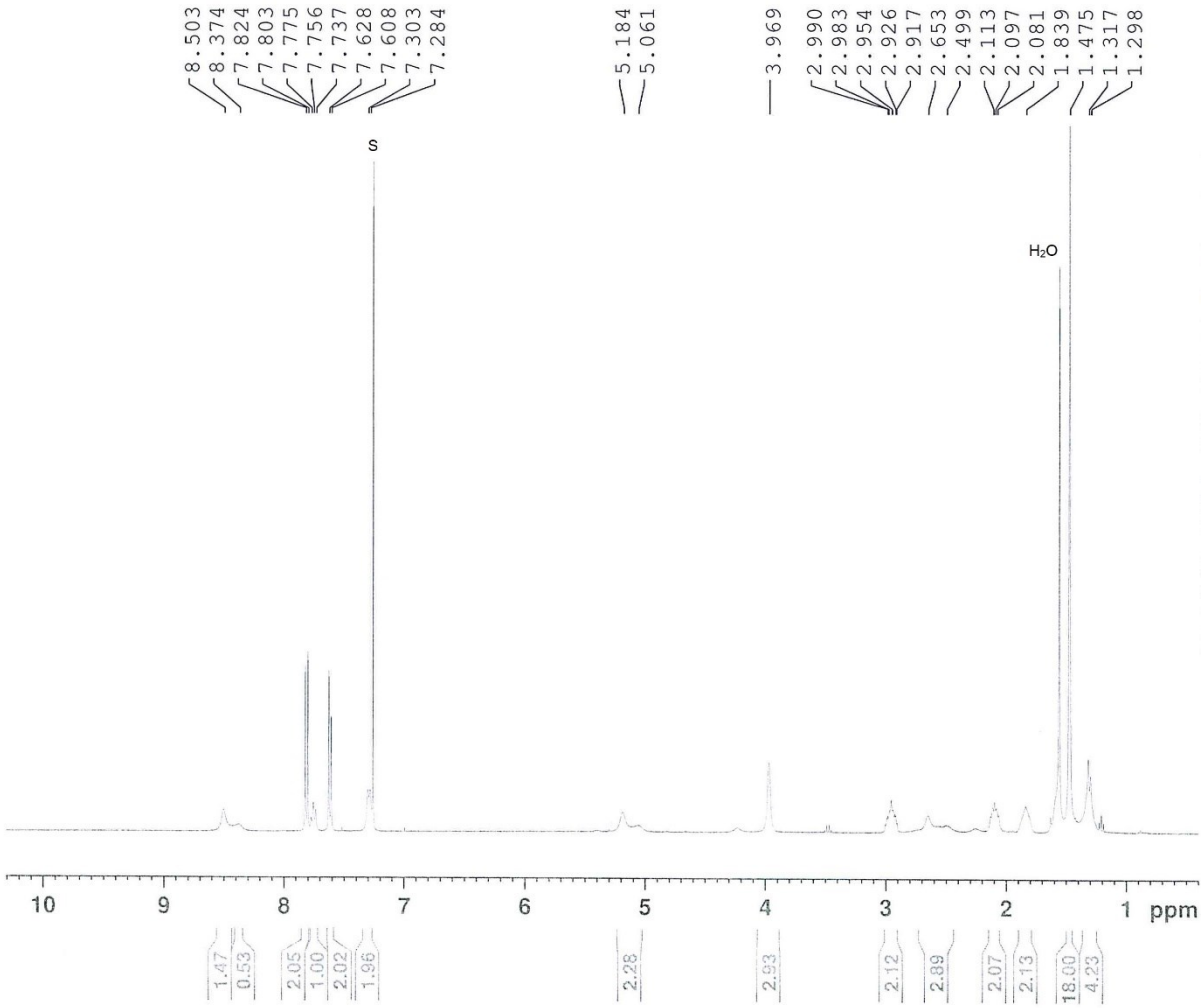

Figure S26. ^{1}H NMR (400 MHz, 298 K, $CDCl_3$) spectrum of **3** (S = residual solvent).

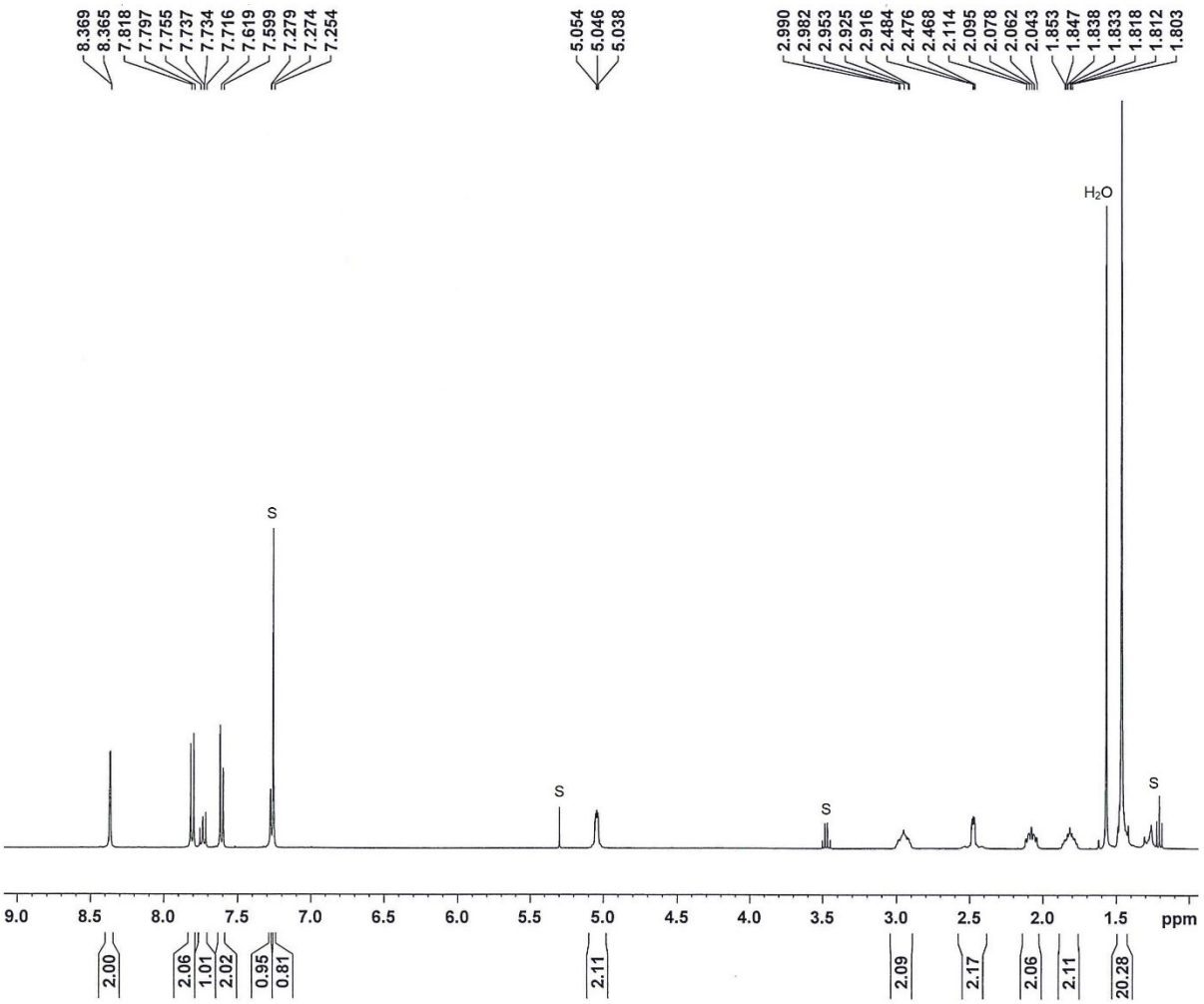

Figure S27. ^{1}H NMR (400 MHz, 298 K, $CDCl_3$) spectrum of **4** (S = residual solvent).

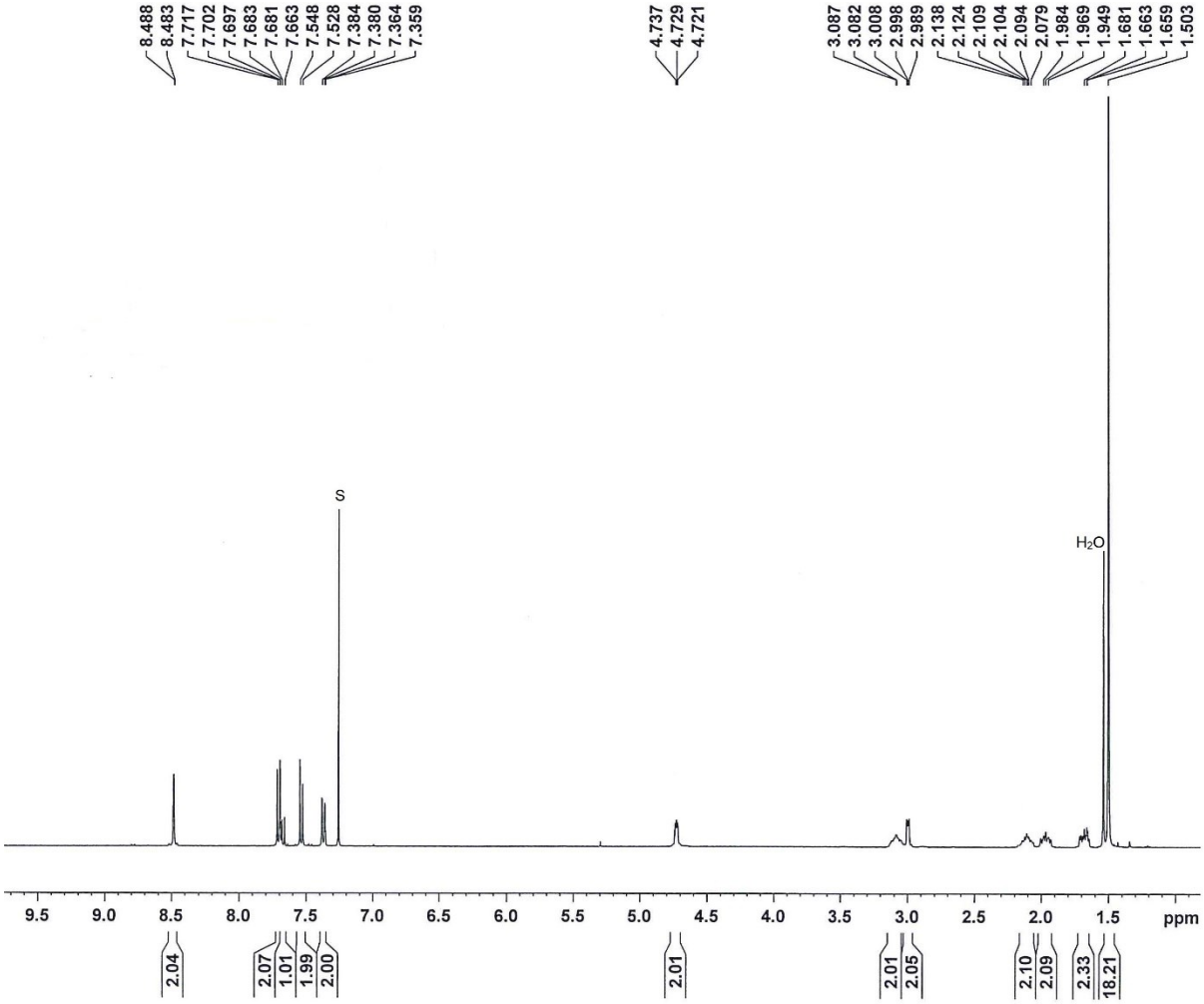

Figure S28. ^{1}H NMR (400 MHz, 298 K, $CDCl_3$) spectrum of **5·HgCl$_2$** (S = residual solvent).

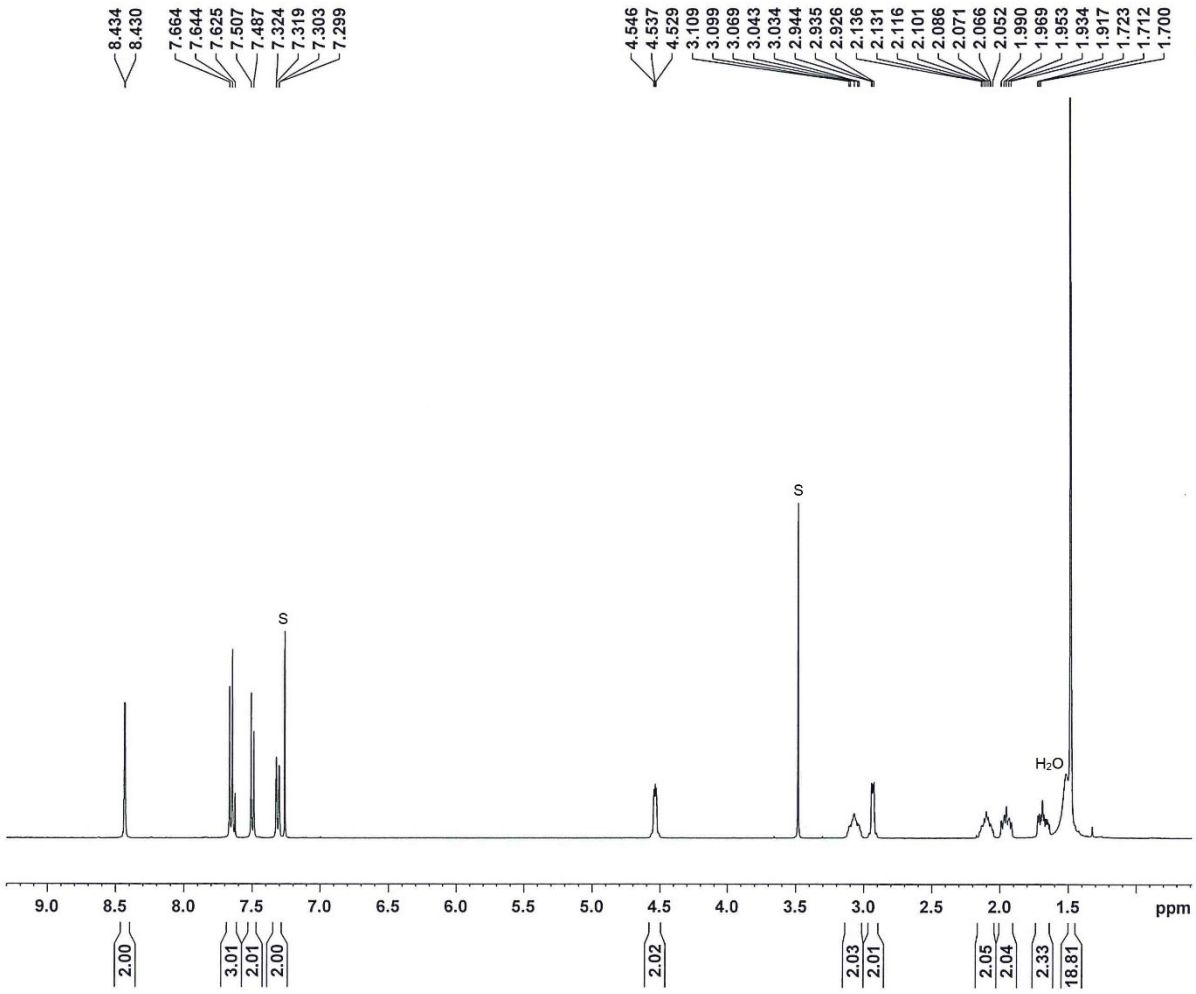

Figure S29. ^{1}H NMR (400 MHz, 298 K, $CDCl_3$) spectrum of **5** (S = residual solvent).

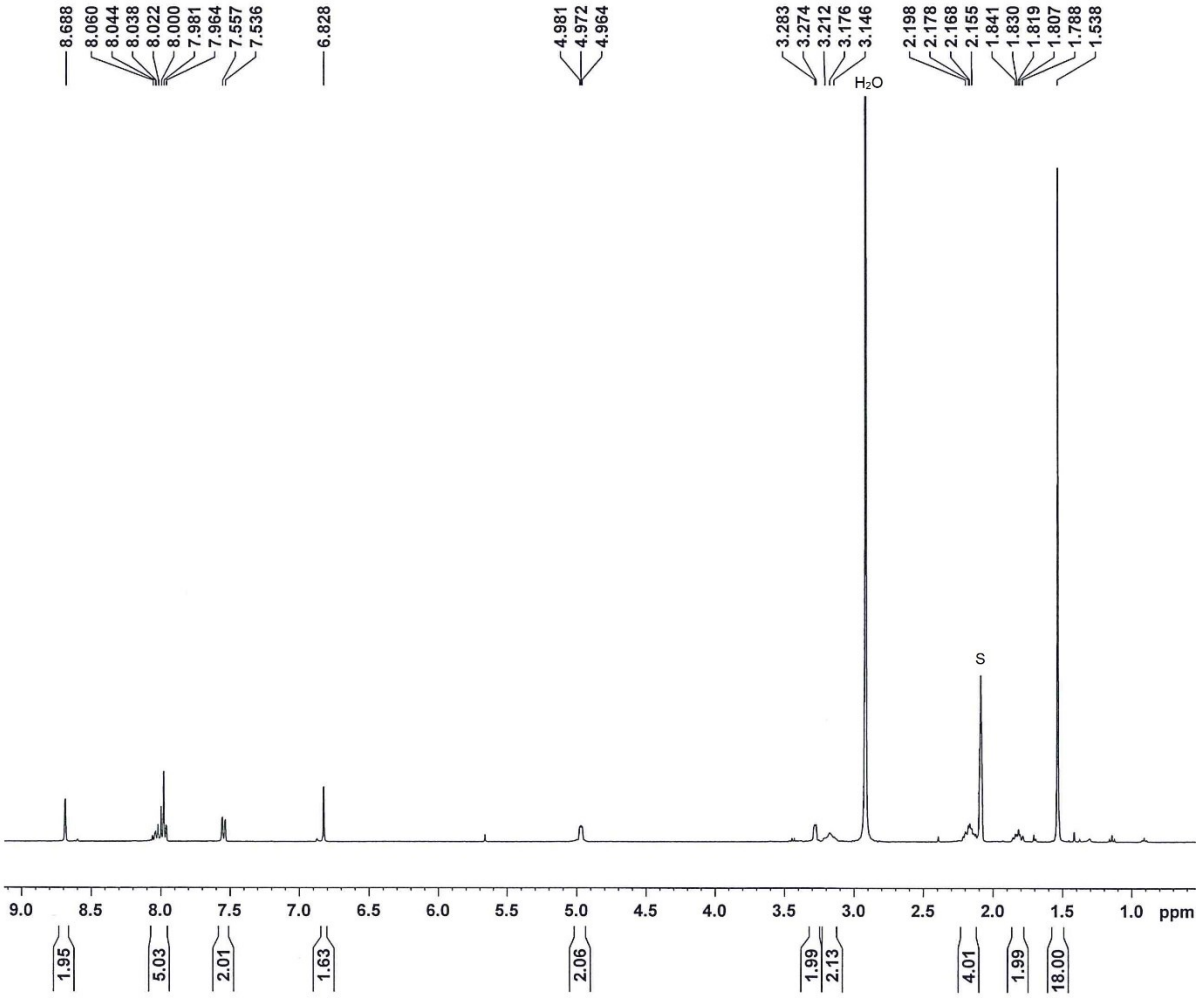

Figure S30. ^{1}H NMR (400 MHz, 298 K, acetone-d_6) spectrum of **6** (S = residual solvent).

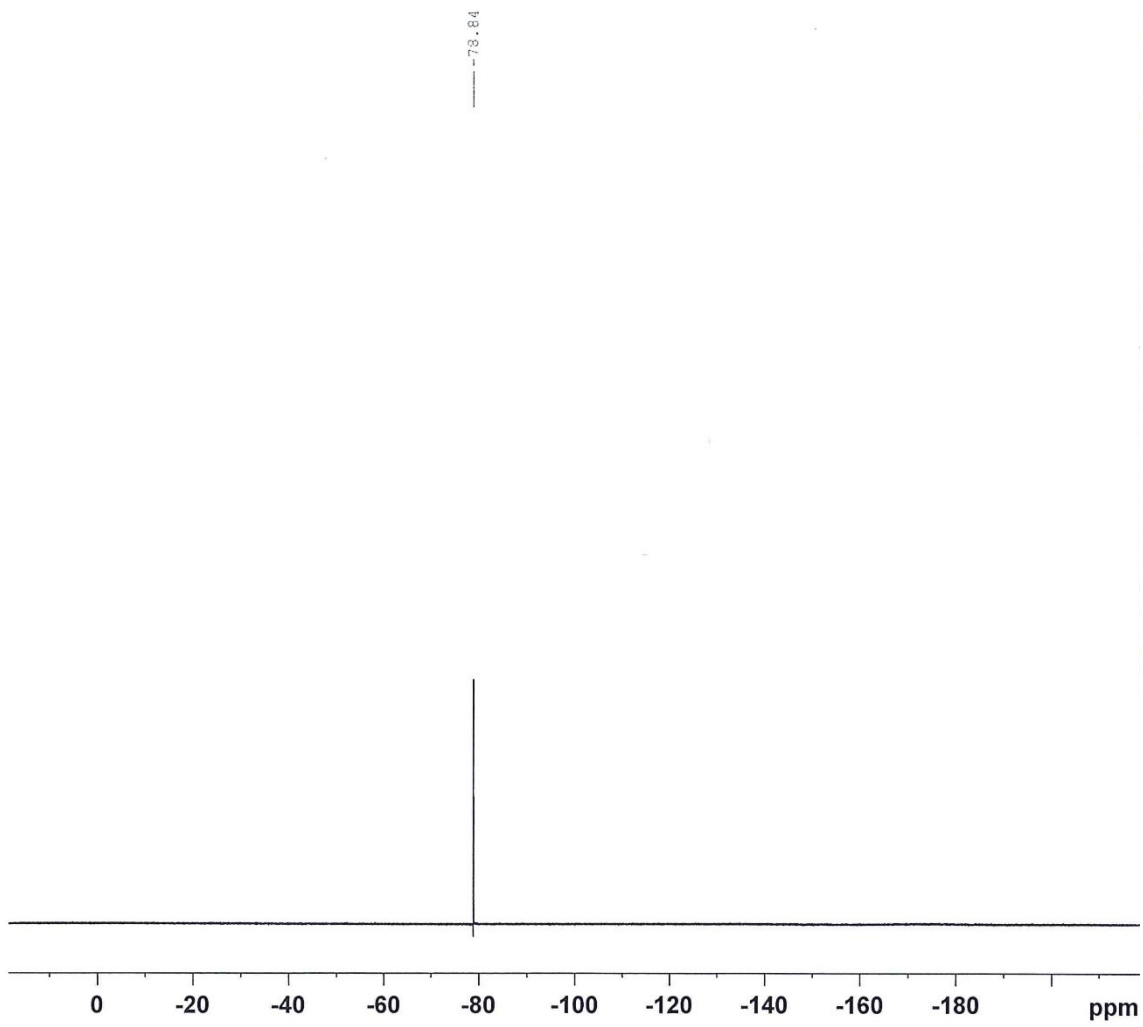

Figure S31. $^{19}F\{^{1}H\}$ NMR (376.5 MHz, 298 K, acetone-d_6) spectrum of **6**.

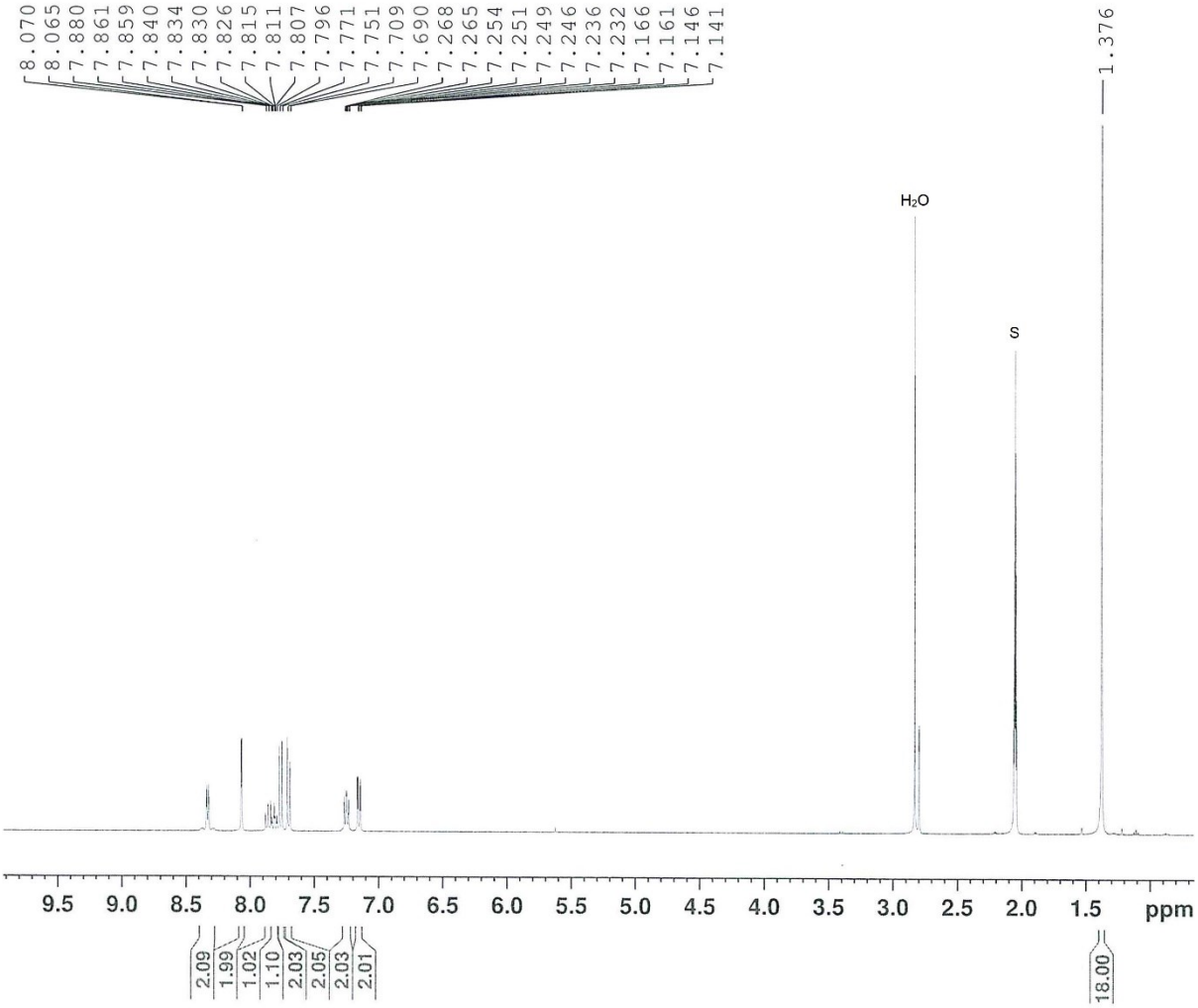

Figure S32. ^{1}H NMR (400 MHz, 298 K, acetone-d_6) spectrum of **7** (S = residual solvent).

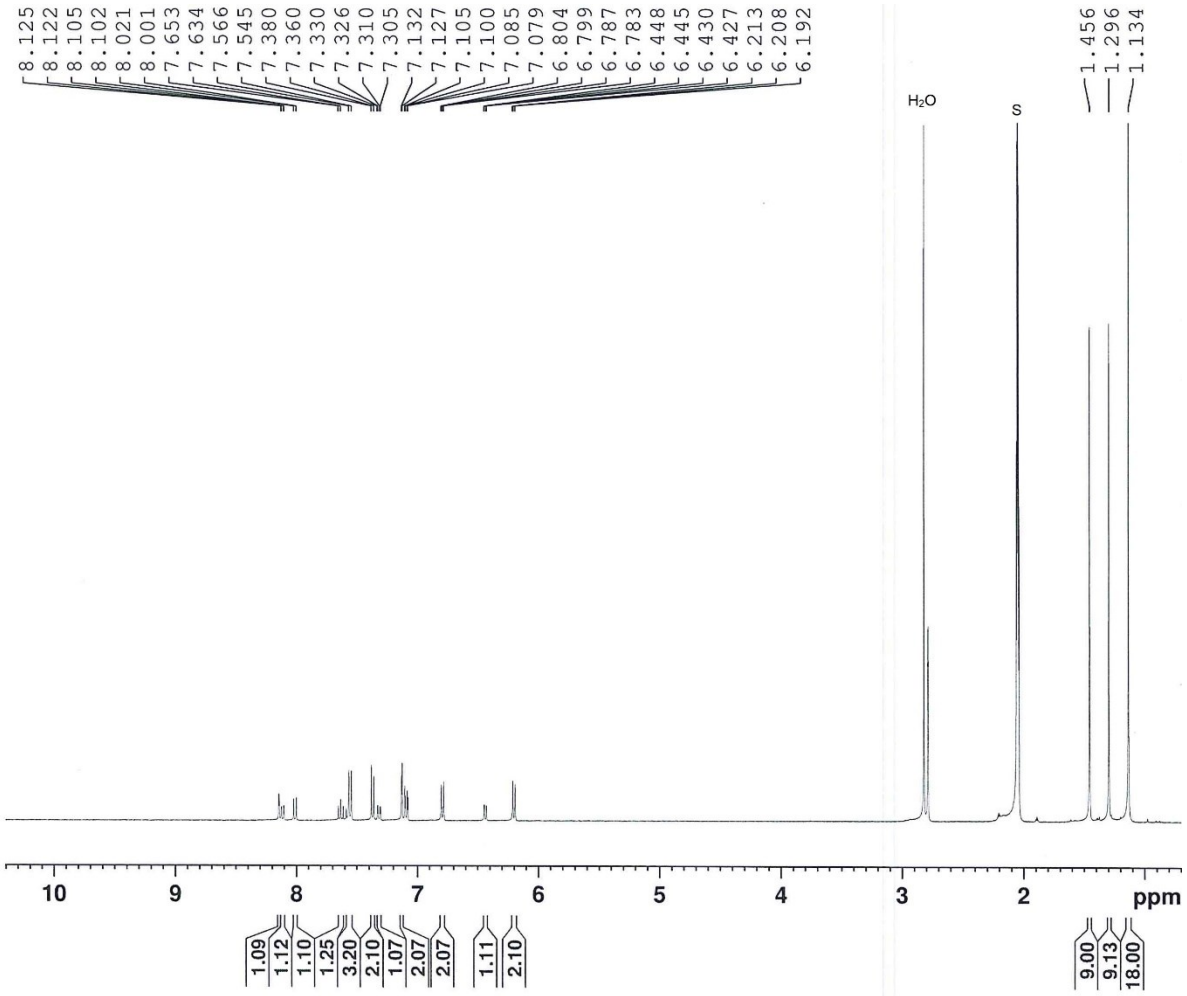

Figure S33. ^{1}H NMR (400 MHz, 298 K, acetone-d_6) spectrum of **8** (S = residual solvent).

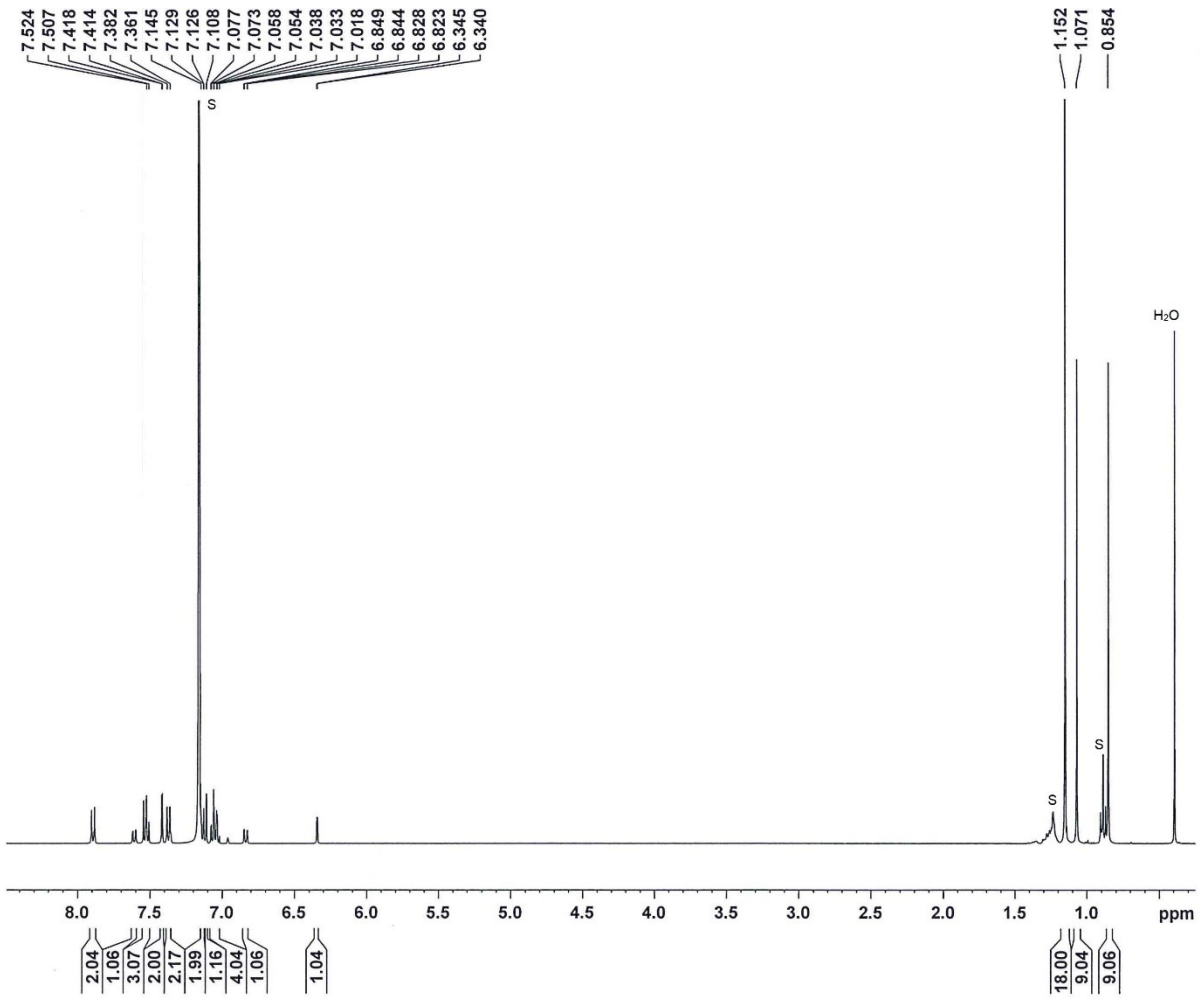

Figure S34. ^{1}H NMR (400 MHz, 298 K, $CDCl_3$) spectrum of **8'** (S = residual solvent).

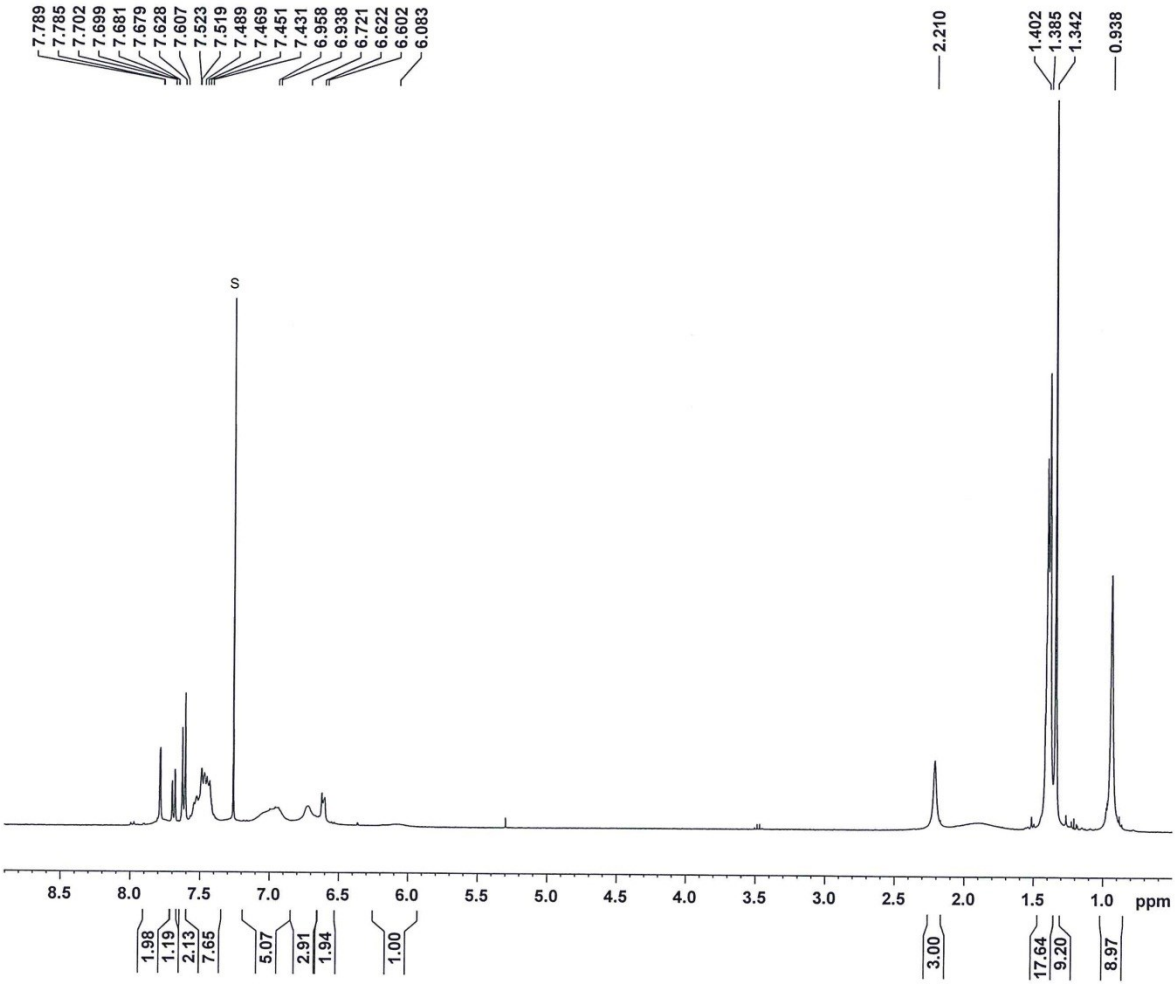

Figure S35. ^{1}H NMR (400 MHz, 298 K, $CDCl_3$) spectrum of **9** (S = residual solvent).

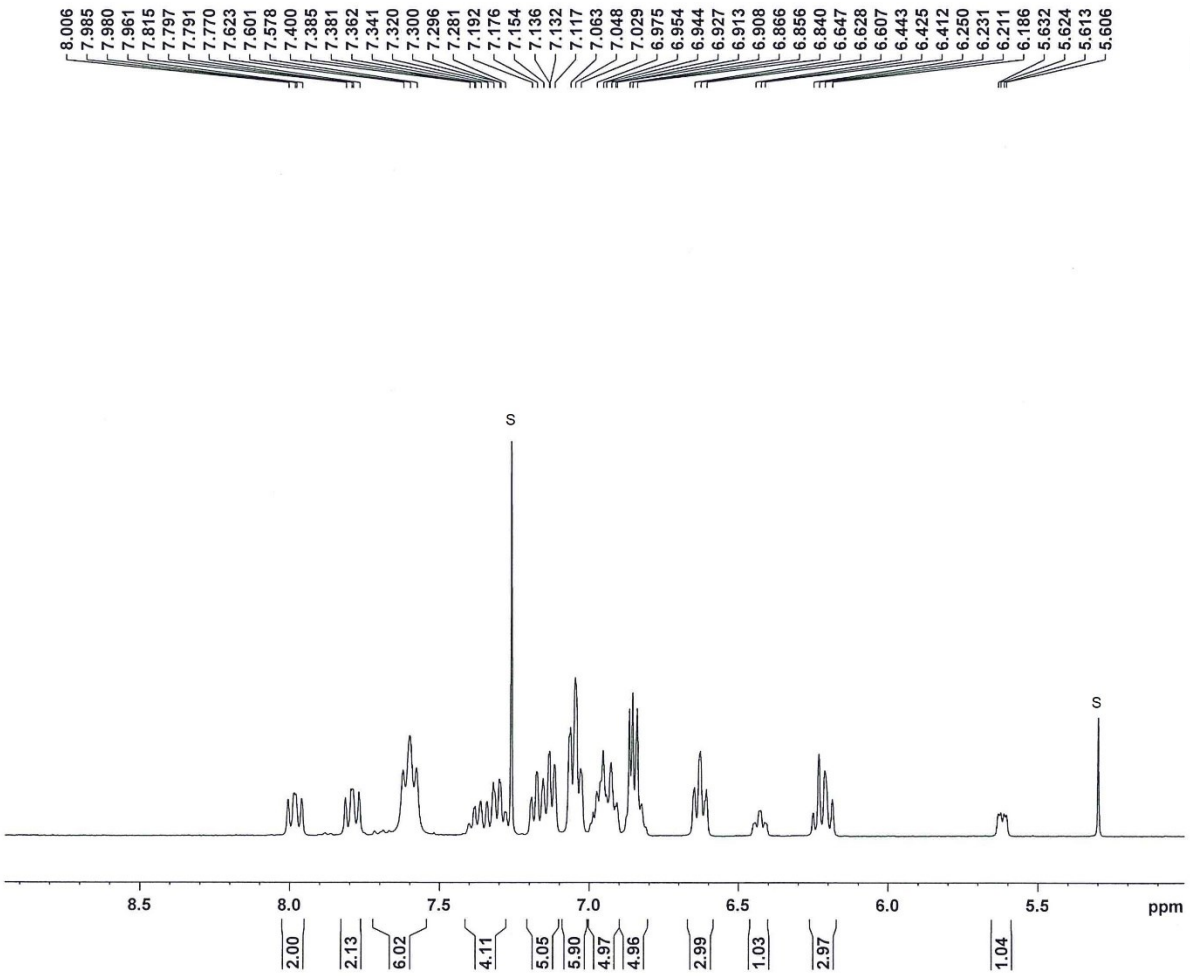

Figure S36. ^{1}H NMR (400 MHz, 298 K, $CDCl_3$) spectrum of **10** (S = residual solvent).

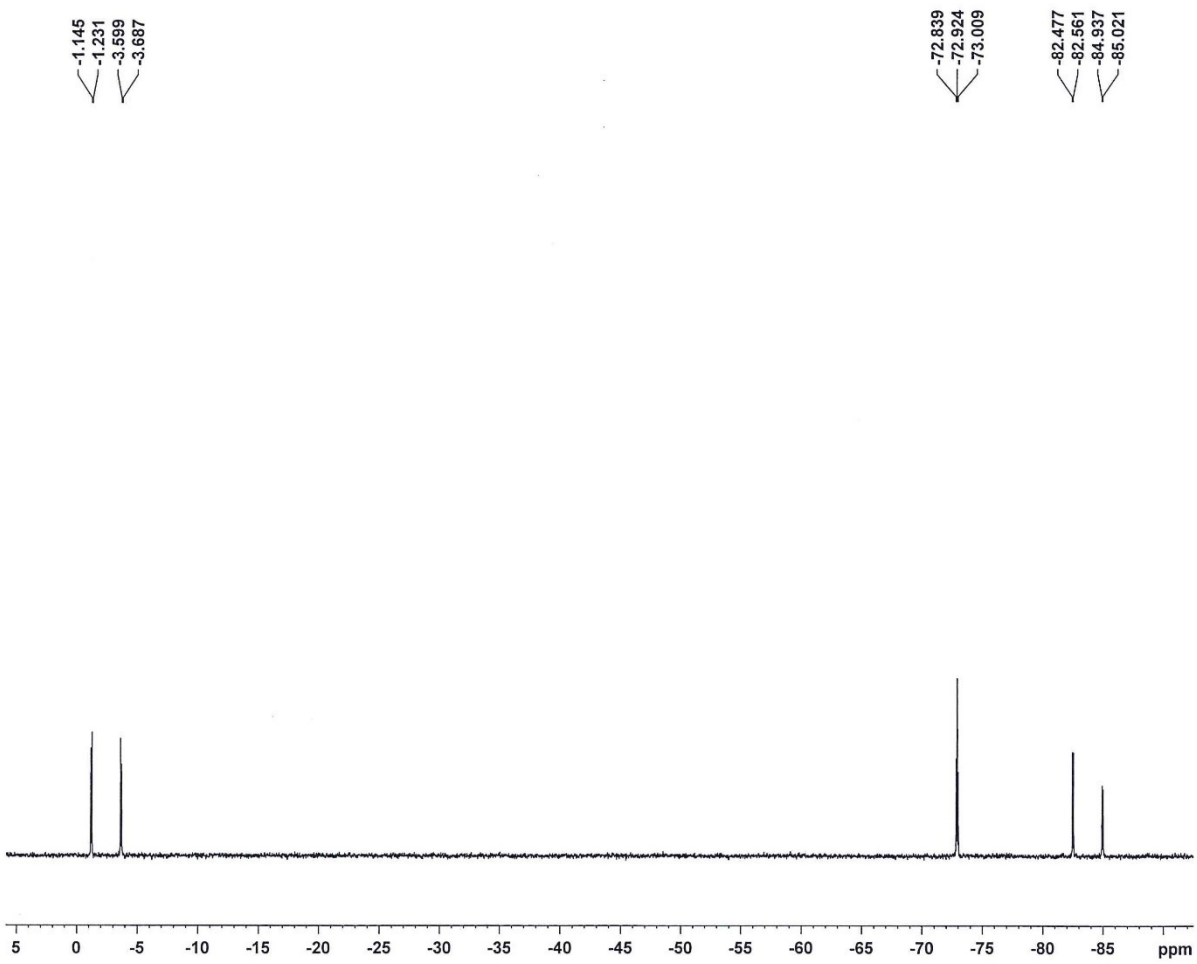

Figure S37. $^{31}P\{^{1}H\}$ NMR (162 MHz, 298 K, $CDCl_3$) spectrum of **10**.

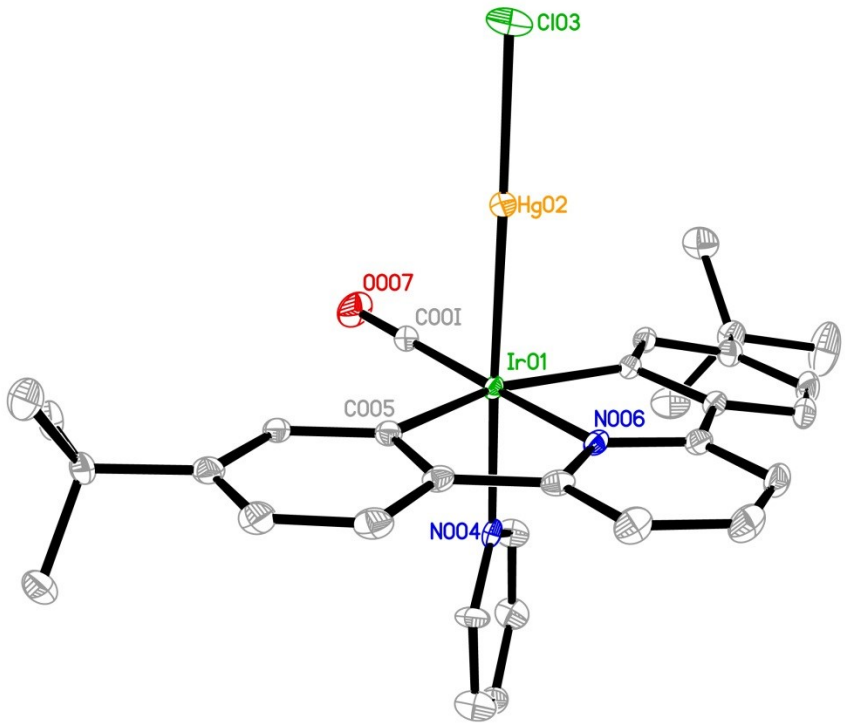

Figure S38. Preliminary x-ray structure of [Ir(C^N^C)(HgCl)(CO)(py)] (**7**).

Figure S39. Molecular structure of [Cl(κ²*C,N*-HC^N^C)(cod)IrHgIr(cod)Cl_2]$_2$ (**2**). The ellipsoids are drawn at 30% probability level.

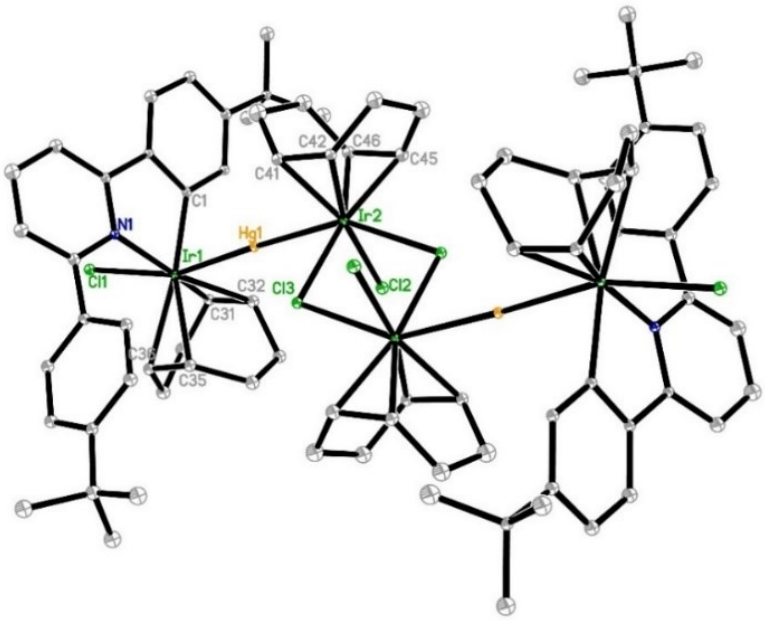

Table S2. Selected bond lengths and angles of [Cl(κ²*C,N*-HC^N^C)(cod)IrHgIr(cod)Cl_2]$_2$ (**2**).

Ir1-Hg1	2.5829(3)	Ir2-Hg1	2.6314(3)
Ir1-C1	2.047(6)	Ir1-N1	2.182(4)
Ir1-C31	2.161(6)	Ir1-C32	2.207(6)
Ir1-C35	2.349(6)	Ir1-C36	2.310(6)
Ir1-Cl1	2.4694(13)	Ir2-Cl2	2.3950(13)
Ir2-Cl3	2.4126(12)	Ir2-C41	2.162(6)
Ir2-C42	2.159(5)	Ir2-C45	2.127(6)
Ir2-C46	2.156(6)	C31-C32	1.400(9)
C35-C36	1.374(9)	C41-C42	1.399(8)
C45-C46	1.411(9)		
C1-Ir1-N1	79.4(2)	C1-Ir1-Cl1	86.91(16)
C1-Ir1-C31	91.7(2)	C1-Ir1-C32	94.0(2)
C1-Ir1-C35	159.8(2)	C1-Ir1-C36	164.9(2)
C1-Ir1-Hg1	79.14(15)	N1-Ir1-Cl1	78.75(13)
N1-Ir1-C31	159.2(2)	N1-Ir1-C32	160.6(2)
N1-Ir1-C35	102.65(19)	N1-Ir1-C36	105.16(19)
N1-Ir1-Hg1	84.78(12)	Cl1-Ir1-C31	81.99(16)
Cl1-Ir1-C32	119.36(16)	Cl1-Ir1-C35	113.27(15)
Cl1-Ir1-C36	80.07(16)	Cl1-Ir1-Hg1	79.14(15)
C31-Ir1-C32	37.4(2)	C31-Ir1-C35	92.2(2)
C31-Ir1-C36	79.0(2)	C31-Ir1-Hg1	112.27(16)
C32-Ir1-C35	77.4(2)	C32-Ir1-C36	85.9(2)
C32-Ir1-Hg1	76.07(16)	C35-Ir1-C36	34.3(2)
C35-Ir1-Hg1	81.03(15)	C36-Ir1-Hg1	115.31(15)
Ir1-Hg1-Ir2	176.587(11)	Cl2-Ir2-Cl3	91.66(5)
Cl2-Ir2-Cl3^{1}	85.44(4)	Cl2-Ir2-C41	155.93(16)
Cl2-Ir2-C42	165.74(16)	Cl2-Ir2-C45	89.64(17)

Cl2-Ir2-C46	89.64(17)	Cl2-Ir2-Hg1	76.14(3)
Cl3-Ir2-Cl3^{1}	80.68(4)	Cl3-Ir2-C41	88.87(17)
Cl3-Ir2-C42	92.91(16)	Cl3-Ir2-C45	164.70(17)
Cl3-Ir2-C46	156.75(17)	Cl3-Ir2-Hg1	78.67(3)
Cl3^{1}-Ir2-C41	118.34(16)	Cl3^{1}-Ir2-C42	81.99(16)
Cl3^{1}-Ir2-C45	84.23(17)	Cl3^{1}-Ir2-C46	122.55(17)
Cl3^{1}-Ir2-Hg	151.75(3)	C41-Ir2-C42	37.8(2)
C41-Ir2-C45	96.1(2)	C41-Ir2-C46	80.7(2)
C41-Ir2-Hg1	80.39(16)	C45-Ir2-C46	38.5(2)
C45-Ir2-Hg1	116.39(17)	C46-Ir2-Hg1	79.12(17)

Figure S40. Molecular structure of [(C^N^C)(cod)IrHgIr(cod)Cl_2] (**3**). The ellipsoids are drawn at 30% probability level.

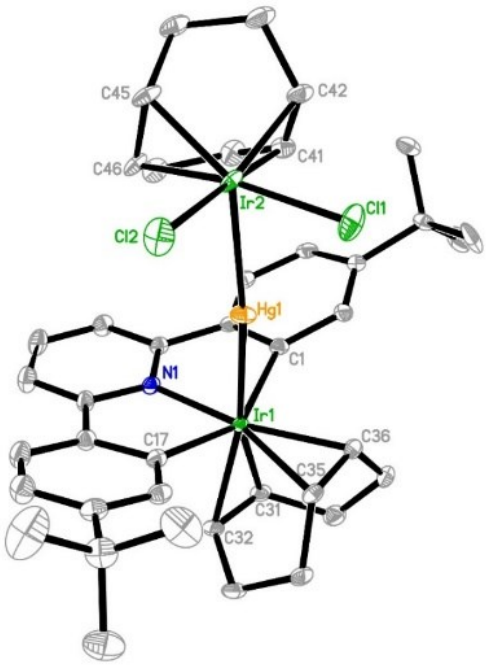

Table S3. Selected bond lengths and angles of [(C^N^C)(cod)IrHgIr(cod)Cl_2] (**3**).

Ir1-N1	2.045(3)	Ir1-C1	2.126(4)
Ir1-C17	2.131(4)	Ir1-C31	2.211(4)
Ir1-C32	2.187(4)	Ir1-C35	2.180(4)
Ir1-C36	2.170(4)	Ir1-Hg1	2.5841(3)
Ir2-Cl1	2.3335(12)	Ir2-Cl2	2.256(3)
Ir2-C41	2.133(5)	Ir2-C42	2.191(11)
Ir2-C45	2.146(10)	Ir2-C46	2.101(11)
Ir2-Hg1	2.6656(3)	C31-C32	1.426(6)
C35-C36	1.417(7)	C41-C42	1.294(11)
C45-C46	1.422(15)		
N1-Ir1-C1	77.30(15)	N1-Ir1-C17	77.99(15)
N1-Ir1-C31	92.65(15)	N1-Ir1-C32	88.86(15)
N1-Ir1-C35	160.94(16)	N1-Ir1-C36	160.32(17)
N1-Ir1-Hg1	90.67(10)	C1-Ir1-C17	148.08(16)
C1-Ir1-C31	83.44(16)	C1-Ir1-C32	119.22(16)
C1-Ir1-C35	121.70(17)	C1-Ir1-C36	83.89(17)
C1-Ir1-Hg1	81.20(11)	C17-Ir1-C31	117.65(16)
C17-Ir1-C32	80.04(16)	C17-Ir1-C35	84.61(17)
C17-Ir1-C36	121.66(17)	C17-Ir1-Hg1	79.19(11)
C31-Ir1-C32	37.84(16)	C31-Ir1-C35	88.54(18)
C31-Ir1-C36	79.34(18)	C31-Ir1-Hg1	163.16(11)
C32-Ir1-C35	80.45(17)	C32-Ir1-C36	95.36(17)
C32-Ir1-Hg1	158.85(12)	C35-Ir1-C36	38.03(17)
C35-Ir1-Hg1	93.67(13)	C36-Ir1-Hg1	92.16(13)
Ir1-Hg1-Ir2	169.439(9)	Cl1-Ir2-Cl2	93.44(10)

Cl1-Ir2-C41	91.67(14)	Cl1-Ir2-C42	84.1(3)
Cl1-Ir2-C45	153.1(3)	Cl1-Ir2-C46	165.9(3)
Cl1-Ir2-Hg1	79.68(4)	Cl2-Ir2-C41	168.61(17)
Cl2-Ir2-C42	156.1(3)	Cl2-Ir2-C45	93.7(3)
Cl2-Ir2-C46	91.6(3)	Cl2-Ir2-Hg1	89.05(12)
C41-Ir2-C42	34.8(3)	C41-Ir2-C45	86.3(3)
C41-Ir2-C46	81.1(3)	C41-Ir2-Hg1	81.85(12)
C42-Ir2-C45	79.0(4)	C42-Ir2-C46	96.5(4)
C42-Ir2-Hg1	113.7(3)	C45-Ir2-C46	39.1(4)
C45-Ir2-Hg1	126.3(3)	C46-Ir2-Hg1	87.3(3)

Figure S41. Molecular structure of [Ir(C^N^C)(cod)(HgCl)] (**4**). The ellipsoids are drawn at 30% probability level.

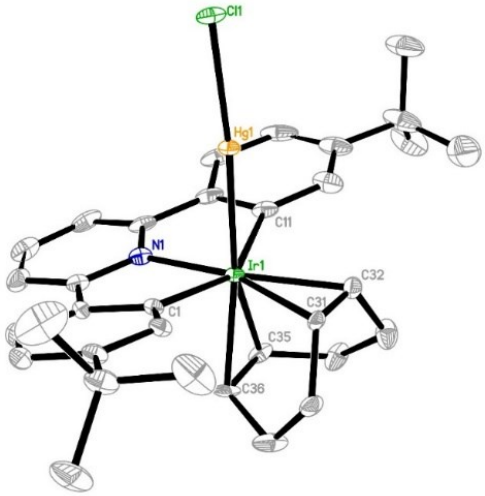

Table S4. Selected bond lengths and angles of [Ir(C^N^C)(cod)(HgCl)] (**4**).

Ir1-N1	2.040(5)	Ir1-C1	2.147(6)
Ir1-C11	2.148(6)	Ir1-C31	2.180(6)
Ir1-C32	2.194(6)	Ir1-C35	2.202(6)
Ir1-C36	2.216(6)	Ir1-Hg1	2.5705(3)
Hg1-Cl1	2.4255(13)	C31-C32	1.398(9)
C35-C36	1.395(9)		
N1-Ir1-C1	77.2(2)	N1-Ir1-C11	78.1(2)
N1-Ir1-C31	159.9(2)	N1-Ir1-C32	161.7(2)
N1-Ir1-C35	90.2(2)	N1-Ir1-C36	90.7(2)
N1-Ir1-Hg1	91.68(13)	C1-Ir1-C11	150.3(2)
C1-Ir1-C31	83.7(2)	C1-Ir1-C32	120.8(2)
C1-Ir1-C35	117.0(2)	C1-Ir1-C36	81.2(2)
C1-Ir1-Hg1	82.71(14)	C11-Ir1-C31	122.0(3)
C11-Ir1-C32	85.2(3)	C11-Ir1-C35	79.3(2)
C11-Ir1-C36	115.4(2)	C11-Ir1-Hg1	81.74(17)
C31-Ir1-C32	37.3(2)	C31-Ir1-C35	92.6(2)
C31-Ir1-C36	79.8(2)	C31-Ir1-Hg1	92.35(15)
C32-Ir1-C35	79.2(2)	C32-Ir1-C36	89.6(3)
C32-Ir1-Hg1	93.33(17)	C35-Ir1-C35	36.8(2)
C35-Ir1-Hg1	160.14(18)	C36-Ir1-Hg1	162.79(18)
Ir1-Hg1-Cl1	171.64(4)		

Figure S42. Molecular structure of [Ir(C^N^C)(cod)Cl] (**5**). The ellipsoids are drawn at 30% probability level.

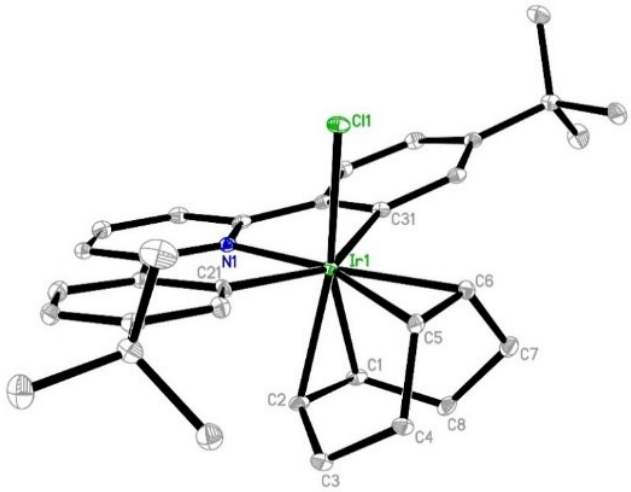

Table S5. Selected bond lengths and angles of [Ir(C^N^C)(cod)Cl] (**5**).

Ir1-N1	2.052(2)	Ir1-C2l	2.140(3)
Ir1-C31	2.139(3)	Ir1-C1	2.177(3)
Ir1-C2	2.168(3)	Ir1-C5	2.178(3)
Ir1-C6	2.181(3)	Ir1-Cl1	2.3993(6)
C1-C2	1.402(4)	C5-C6	1.405(4)
N1-Ir1-C21	77.92(10)	N1-Ir1-C31	77.45(10)
N1-Ir1-C1	90.01(10)	N1-Ir1-C2	87.10(10)
N1-Ir1-C5	160.61(10)	N1-Ir1-C6	160.15(10)
N1-Ir1-Cl1	96.06(6)	C21-Ir1-C31	151.35(10)
C21-Ir1-C1	113.74(10)	C21-Ir1-C2	76.45(10)
C21-Ir1-C5	84.68(10)	C21-Ir1-C6	121.81(11)
C21-Ir1-Cl1	83.26(7)	C31-Ir1-C1	80.68(10)
C31-Ir1-C2	116.53(10)	C31-Ir1-C5	121.47(10)
C31-Ir1-C6	83.92(11)	C31-Ir1-Cl1	85.01(7)
C1-Ir1-C2	37.65(11)	C1-Ir1-C5	89.20(10)
C1-Ir1-C6	80.18(11)	C1-Ir1-Cl1	162.86(8)
C2-Ir1-C5	80.49(10)	C2-Ir1-C6	95.25(10)
C2-Ir1-Cl1	158.34(8)	C5-Ir1-C6	37.61(10)
C5-Ir1-Cl1	90.27(7)	C6-Ir1-Cl1	89.01(8)

Figure S43. Molecular structure of [Ir(C^N^C)(κ²*C,N*-HC^N^C)(CO)] (**8**). The ellipsoids are drawn at 30% probability level.

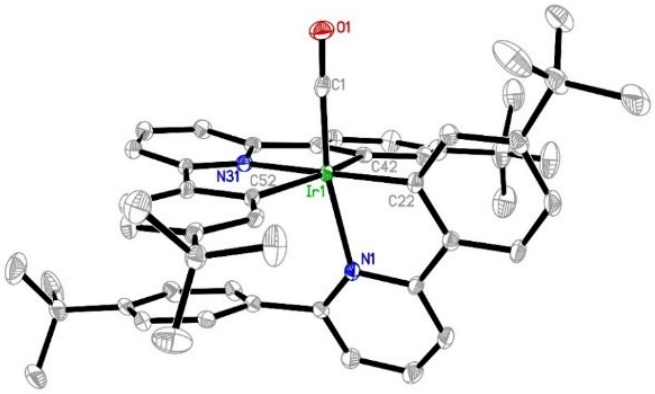

Table S6. Selected bond lengths and angles of [Ir(C^N^C)(κ²*C,N*-HC^N^C)(CO)] (**8**).

Ir1-N1	2.163(2)	Ir1-N31	2.083(2)
Ir1-C1	1.821(3)	Ir1-C22	2.028(3)
Ir1-C42	2.101(3)	Ir1-C52	2.113(3)
C1-O1	1.153(3)		
N1-Ir1-N31	99.57(8)	N1-Ir1-C1	168.35(10)
N1-Ir1-C22	79.57(10)	N1-Ir1-C42	81.98(9)
N1-Ir1-C52	97.15(9)	N31-Ir1-C1	91.02(10)
N31-Ir1-C22	176.42(10)	N31-Ir1-C42	78.94(10)
N31-Ir1-C52	79.14(9)	C1-Ir1-C22	89.56(11)
C1-Ir1-C42	95.41(11)	C1-Ir1-C52	89.57(11)
C22-Ir1-C42	97.49(10)	C22-Ir1-C52	104.40(10)
C42-Ir1-C52	157.59(10)	Ir1-C1-O1	176.8(2)

Figure S44. Molecular structure of the isomer **8'**. The ellipsoids are drawn at 30% probability level.

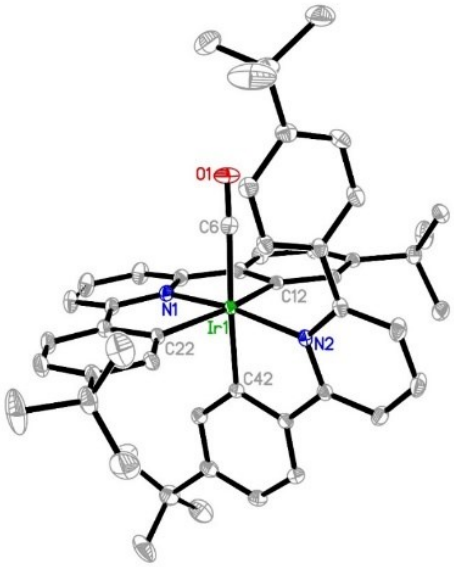

Table S7. Selected bond lengths and angles of the isomer **8'**.

Ir1-N1	2.0122(17)	Ir1-N2	2.0998(16)
Ir1-C6	1.933(2)	Ir1-C12	2.096(2)
Ir1-C22	2.114(2)	Ir1-C42	2.060(2)
C6-O1	1.135(3)		
N1-Ir1-N2	168.31(7)	N1-Ir1-C6	90.16(8)
N1-Ir1-C12	80.17(8)	N1-Ir1-C22	80.02(8)
N1-Ir1-C42	89.19(8)	N2-Ir1-C6	100.56(8)
N2-Ir1-C12	95.48(7)	N2-Ir1-C22	103.07(7)
N2-Ir1-C42	79.73(7)	C6-Ir1-C12	87.71(8)
C6-Ir1-C22	96.91(8)	C6-Ir1-C42	174.97(8)
C12-Ir1-C22	159.66(8)	C12-Ir1-C42	87.27(8)
C22-Ir1-C42	87.89(8)	Ir1-C6-O1	170.77(19)

Figure S45. Molecular structure of [Ir(κ^2*C,N*-HC^N^C)$_2$(OTs)(CO)] (**9**). The ellipsoids are drawn at 30% probability level.

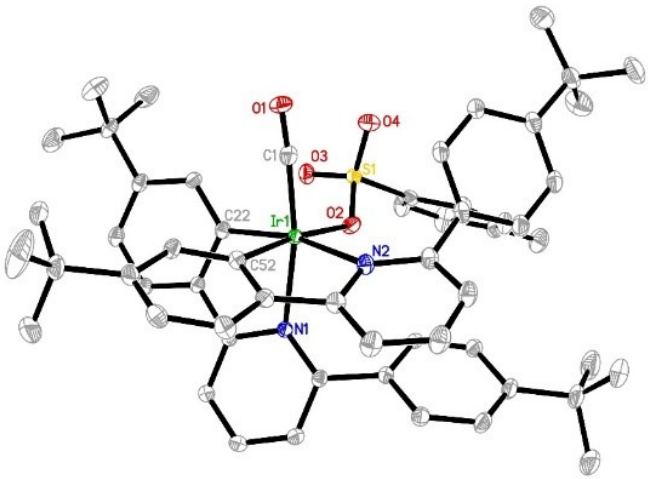

Table S8. Selected bond lengths and angles of [Ir(κ^2*C,N*-HC^N^C)$_2$(OTs)(CO)] (**9**).

Ir1-N1	2.172(2)	Ir1-N2	2.274(2)
Ir1-C1	1.844(3)	Ir1-C22	2.032(3)
Ir1-C52	2.022(3)	Ir1-O2	2.1914(19)
C1-O1	1.138(4)		
N1-Ir1-N2	90.59(8)	N1-Ir1-C1	169.77(10)
N1-Ir1-C22	80.35(9)	N1-Ir1-C52	84.62(9)
N1-Ir1-O2	88.17(8)	N2-Ir1-C1	96.44(10)
N2-Ir1-C22	164.67(9)	N2-Ir1-C52	78.28(10)
N2-Ir1-O2	101.50(8)	C1-Ir1-C22	91.14(11)
C1-Ir1-C52	89.52(12)	C1-Ir1-O2	97.67(10)
C22-Ir1-C52	88.51(10)	C22-Ir1-O2	90.63(9)
C52-Ir1-O2	172.78(9)		

Figure S46. Molecular structure of [Ir(PPh$_3$)(κ^2*P,C*-C$_6$H$_4$PPh$_2$)$_2$Cl] (**10**). The ellipsoids are drawn at 30% probability level.

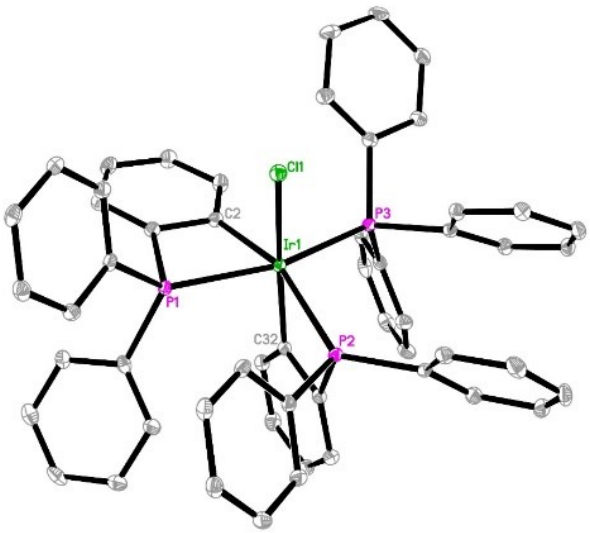

Table S9. Selected bond lengths and angles of [Ir(PPh$_3$)(κ^2*P,C*-C$_6$H$_4$PPh$_2$)$_2$Cl] (**10**).

Ir1-Cl1	2.4921(8)	Ir1-C2	2.079(3)
Ir1-C32	2.044(4)	Ir1-P1	2.3935(8)
Ir1-P2	2.3937(8)	Ir1-P3	2.3300(8)
Cl1-Ir1-C2	95.18(10)	Cl1-Ir1-C32	167.47(10)
Cl1-Ir1-P1	87.73(3)	Cl1-Ir1-P2	100.01(3)
Cl1-Ir1-P3	94.51(3)	C2-Ir1-C32	95.77(13)
C2-Ir1-P1	67.28(9)	C2-Ir1-P2	160.24(10)
C2-Ir1-P3	93.58(9)	C32-Ir1-P1	90.88(9)
C32-Ir1-P2	68.01(10)	C32-Ir1-P3	90.88(9)
P1-Ir1-P2	100.61(3)	P1-Ir1-P3	160.86(3)
P2-Ir1-P3	97.72(3)		

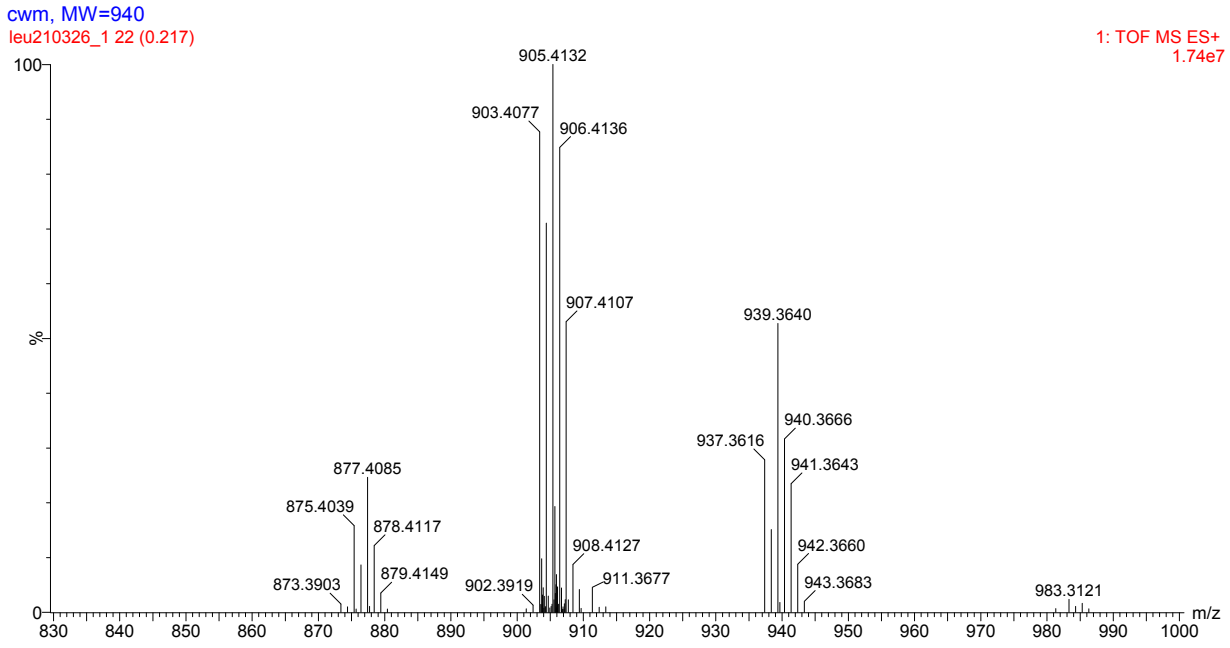

Figure S47. Mass spectrum (ESI) of the product of oxidation of **8** by $(4\text{-}BrC_6H_4)_3NSbCl_6$.